

Design and Optimization of Pyrazinecarboxamide-Based Inhibitors of Diacylglycerol Acyltransferase 1 (DGAT1) Leading to a Clinical Candidate Dimethylpyrazinecarboxamide Phenylcyclohexylacetic Acid (AZD7687)

Jonas G. Barlind,[†] Udo A. Bauer,[†] Alan M. Birch,[‡] Susan Birtles,[‡] Linda K. Buckett,[‡] Roger J. Butlin,[‡] Robert D. M. Davies,[‡] Jan W. Eriksson,^{†,§} Clare D. Hammond,[‡] Ragnar Hovland,[†] Petra Johannesson,^{*,†} Magnus J. Johansson,[†] Paul D. Kemmitt,[‡] Bo T. Lindmark,[†] Pablo Morentin Gutierrez,[‡] Tobias A. Noeske,[†] Andreas Nordin,[†] Charles J. O'Donnell,[‡] Annika U. Petersson,[†] Alma Redzic,[†] Andrew V. Turnbull,[‡] and Johanna Vinblad[†]

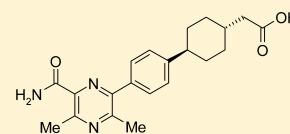
[†]Cardiovascular and Gastrointestinal Innovative Medicines Unit Mölndal, AstraZeneca R&D, S-431 83 Mölndal, Sweden

[‡]AstraZeneca R&D, Alderley Park, Macclesfield, Cheshire, SK10 4TG, U.K.

[§]Department of Molecular and Clinical Medicine, Sahlgrenska University Hospital, S-413 45 Gothenburg, Sweden

Supporting Information

ABSTRACT: A new series of pyrazinecarboxamide DGAT1 inhibitors was designed to address the need for a candidate drug with good potency, selectivity, and physical and DMPK properties combined with a low predicted dose in man. Rational design and optimization of this series led to the discovery of compound **30** (AZD7687), which met the project objectives for potency, selectivity, in particular over ACAT1, solubility, and preclinical PK profiles. This compound showed the anticipated excellent pharmacokinetic properties in human volunteers.



Compound **30** (AZD7687)

hDGAT1 IC₅₀ 0.08 μM

hACAT1 IC₅₀ 34 μM

LogD 0.9

Solubility 700 μM

Half life in human volunteers 9-14 h

INTRODUCTION

Inhibitors of diacylglycerol acyltransferase 1 (DGAT1) have come to the fore in recent years as potential therapies for diabetes, obesity, and other elements of metabolic syndrome.¹ Several accounts of medicinal chemistry optimization programs have been published,^{2–16} and a number of candidate drugs have entered clinical trials.¹

The DGAT1 drug discovery program at AstraZeneca focused initially on the development of a series of oxadiazole substituted phenylcyclohexylacetic acids.¹⁴ Our experience during this work reinforced the significance of the phenylcyclohexylacetic acid side chain in delivering single digit nanomolar potency in conjunction with excellent oral PK properties. This phenylcyclohexylacetic acid side chain is also contained within several other DGAT1 inhibitors, including *trans*-4-[4-[5-[[6-(trifluoromethyl)-3-pyridinyl]amino]-2-pyridinyl]phenyl]cyclohexylacetic acid (LCQ-908),¹⁷ *trans*-4-[4-(4-amino-5-oxo-7,8-dihydropyrimido[5,4-*f*][1,4]oxazepin-6(*5H*)-yl)-phenyl]cyclohexylacetic acid (PF-04620110),⁸ and *trans*-4-[4-(7-aminopyrazolo[1,5-*a*]pyrimidin-6-yl)phenyl]cyclohexylacetic acid (ABT-046),¹⁵ which have all been selected as clinical candidates.^{8,15,18} Our earlier work on oxadiazole substituted phenylcyclohexylacetic acids furthermore informed us of the need for high selectivity for inhibition of DGAT1 over acyl-coenzyme A:cholesterol

acyltransferase 1 (ACAT1) for toxicological (adrenocortical degeneration) reasons, full details of which will be published elsewhere. In addition, we sought to discover a high quality candidate drug, i.e., in terms of current medicinal chemistry thinking it should have relatively low lipophilicity¹⁹ and molecular weight together with high permeability,²⁰ solubility, and general selectivity. A low therapeutic dose was also a key target given the established correlation between this and reduced risk of toxicity in man.²¹ To achieve these goals, we sought to design a compact novel heterocyclic core structure with inherently superior properties on which to attach a suitable lipophilic carboxylic acid appendage.

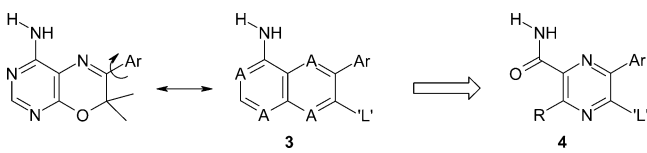
At the time of this work there were two alternative lead structures known. Bayer had published their lipophilic keto acids, for example, **1**,²² and Japan Tobacco/Tularik had together disclosed aminopyrimidinoxazine-based lipophilic acids including the phenylcyclohexylacetic acid **2**.²³ The latter, being less lipophilic, was more interesting to us, and crude overlays were attempted with our oxadiazoles in order to try to understand which were the key elements of the pharmacophore. Our early efforts included use of intermediates including aryl

Received: September 7, 2012

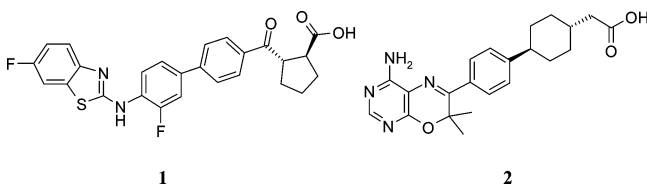
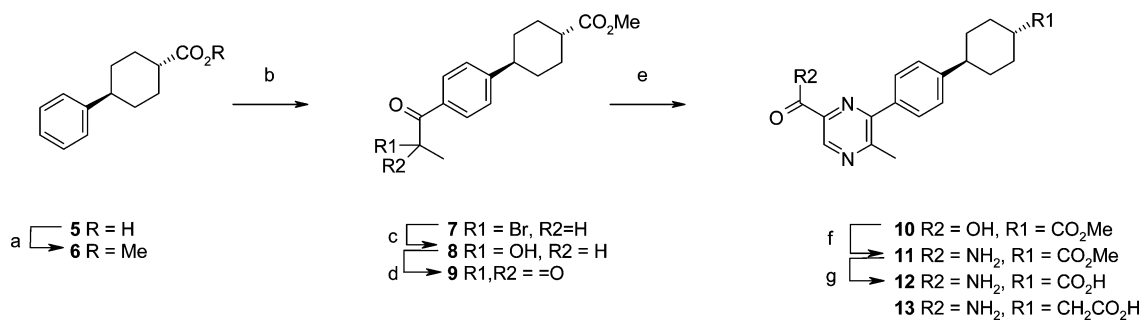
Published: November 2, 2012

halide, triflates, phenacyl halide, and alkynes in multiparallel syntheses, coupling, or cyclocondensing with diverse functionalized/substituted heterocycles or thioamides containing pharmacophoric elements that might be relevant for enzyme inhibition. However, none of these efforts yielded significant inhibitors of DGAT1 (all with IC_{50} of $>10 \mu M$ or with $<20\%$ inhibition at $10 \mu M$). It became clear that the precise arrangement of the pharmacophoric elements in the heterocycle was just as important as the lipophilic acid SAR in delivering enzyme inhibition such that library synthesis from available intermediates was not sufficient in this instance to aid discovery of a new chemical series. A consideration of the low energy conformations of **2** alongside SAR in that series led to the suggestions that (a) the gem-dimethyl in **2** serves to destabilize the coplanar array and hence allow a degree of twisting of the aryl substituent out of the plane of the C=N bond in the oxazine ring (and/or there is a beneficial interaction of this lipophilic region with the enzyme) and (b) the precise H-bonding array of **2** needs to be mimicked in some way. We then hypothesized that a pyrazine ring substituted at C-5 (ortho to the aryl attachment position, C-6) and with a pendent primary carboxamide at C-2 could achieve the key interactions as illustrated in Scheme 1. "L" is a lipophilic group such as methyl or bigger to allow

Scheme 1



the aryl ring to be noncoplanar with the oxazine (**2**) or pyrazine (**3**, **4**) core. "A" is a H-bond acceptor (HBA). The carbonyl oxygen in **4** mimics one pyrimidine N; hence, we need coplanarity of the carboxamide with the pyrazine, and R was chosen to be H in the first iteration because incorporation of a HBA to mimic the other pyrimidine N would likely have an adverse effect on the pyrazinecarboxamide torsion, twisting the CONH₂ group out of the plane of the pyrazine. Bicyclic core **3** was less favored on account of anticipated problems with poor solubility.

Scheme 2^a

^aReagents and conditions: (a) $\text{Me}_3\text{SiCHN}_2$, MeOH, toluene; (b) MeCHBrCOCl , AlCl_3 , DCM, 0°C ; (c) NaOH, DMF, H_2O , rt; (d) 1,1,1-tris(acetoxy)-1,1-dihydro-1,2-benziodoxol-3-(1H)-one ("Dess–Martin periodinane"), DCM, rt; (e) 2,3-diaminopropionic acid hydrochloride, Et_3N , MeOH, rt; (f) (i) EtOCOCl , 4-methylmorpholine, DCM, 0°C , (ii) NH_3/MeOH ; (g) LiOH, MeOH, THF, H_2O , rt.

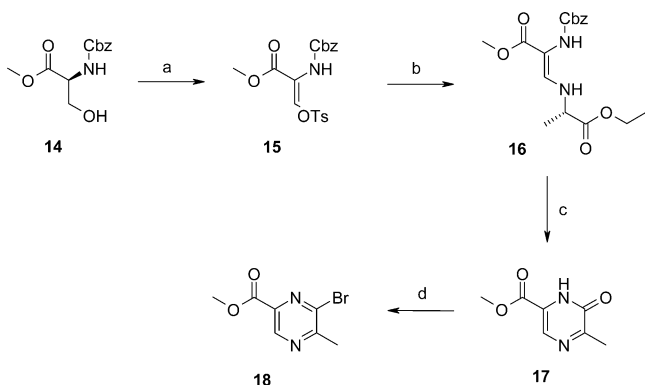
We herein describe the synthesis, structure–activity relationships, and optimization of DGAT1 inhibitors based on the pyrazine carboxamide core structure **4**. This work resulted in the identification of compound **30** as a clinical candidate for the treatment of obesity and metabolic syndrome.

CHEMISTRY

Synthesis of the pyrazine ring was initially achieved via condensation of a diamine with a diketone as shown in Scheme 2. Acid-catalyzed esterification of *trans*-4-phenylcyclohexanecarboxylic acid (**5**) followed by Friedel–Crafts condensation with 2-bromopropionyl chloride furnished bromo ketone **7**. Hydrolysis of the bromide followed by oxidation to diketone **9** and condensation with 2,3-diaminopropionic acid²⁴ gave the pyrazine **10** as a single regioisomer. Conversion to the amide via the mixed anhydride and subsequent ester hydrolysis gave the required pyrazinecarboxamide acid **12**. The same method was initially applied in the synthesis of the homologue **13** with the acetic acid side chain though the yield was poor; hence, we report below only the improved synthesis of this compound (Schemes 5 and 6). In an NMR experiment the proton on the pyrazine ring showed a heteronuclear multiple bond correlation to the pyrazine carbon bearing the methyl in compound **12**, which provided proof that the H and Me are indeed meta-related rather than para as in the unwanted isomer (data not shown).

In the optimization toward new DGAT1 drug candidates we required a convergent synthetic route without any regiochemical ambiguity in the preparation of the substituted pyrazine. Having a lead series consisting of a heterocyclic moiety linked with a phenylcyclohexylacetic acid part, we realized that useful disconnection would be the $\text{Csp}^2\text{--Csp}^2$ between the heterocycle and the phenyl ring. Accordingly, all subsequent efforts were directed toward cross-coupling between these partners, which furthermore allowed for easy variation of both sides. The halogen component was always situated on the heterocycle.

Methyl 6-bromo-5-methylpyrazine-2-carboxylate (**18**) (Scheme 3) was synthesized using a slightly modified procedure to the one described by Pappo et al.²⁵ Commercially available Cbz-L-serine methyl ester (**14**) was subjected to a Swern-type oxidation protocol, followed by trapping of the enolate with tosyl chloride. The resulting Michael acceptor **15** was formally substituted with L-alanine ethyl ester hydrochloride to give intermediate **16**. Upon removal of the benzylcarbamate, spontaneous ring-closure occurred. The reported²⁵ air oxidation (aromatization) of a similar 1,4,5,6-tetrahydropyrazinone failed in our hands. This prompted us to screen other oxidation methods, of which the most

Scheme 3^a

^aReagents and conditions: (a) Et₃N, TsCl, DMSO, DMF, -40 to 0 °C in 2 h; (b) L-Ala-OEt-HCl, Et₃N, MeOH, rt, overnight; (c) (i) Pd/C, NH₄COOH, EtOH, rt, 3 h; (ii) PySO₃ (polymer-bound), DCM, rt, 4 days; (d) POBr₃, toluene, reflux, 8 h.

efficient protocol was the use of polymer-bound pyridinesulfur trioxide. Treatment of **17** with POBr₃ gave the required 6-bromo-5-methylpyrazine-2-carboxylate building block **18**.

The route described above did not allow easy variation in the 3-position. We then relied on the elegant Rh-catalyzed pyrazinone synthesis reported by the Clapham and Janda groups at Scripps.²⁶ Variation of the α -diazo- β -keto esters allowed for the easy access to 3-substituted pyrazinones. The desired α -diazo- β -keto esters were synthesized in a safe manner by the use of polystyrene-supported tosyl azide.²⁷ This synthesis is illustrated in Scheme 4 for the 3,5-dimethyl substituted building block **22**.

The boronic ester intermediate **28** was synthesized starting from commercially available 4-(4'-hydroxyphenyl)cyclohexanone (**24**) (Scheme 5). A Horner–Wadsworth–Emmons reaction between *tert*-butyl (dimethoxyphosphoryl)acetate and the starting ketone provided alkene **25** which was hydrogenated to give a *cis/trans* mixture of phenol **26**, predominantly *trans* (70%). The *trans*-isomer was isolated by chromatography and converted to the triflate **27**. Subsequent palladium-catalyzed coupling with pinacolborane gave the desired boronic ester precursor **28**.

Chloro- or bromopyrazine esters were cross-coupled with boronic ester intermediate **28** using standard Suzuki conditions

(Scheme 6). Pyridine derivatives were prepared in an analogous way. The resulting coupling products were further modified to the final compounds (Tables 1–5) using standard chemistry procedures (see Experimental Section).

The isomeric methylpyrazine compound **31** was prepared analogously (Scheme 7).

Preparation of the propionic acid analogue **61** proceeded by standard homologation chemistry (Scheme 8).

Preparation of the 2-fluoro- and 2-chlorophenylcyclohexane analogues (*cis* and *trans*) (Table 5) proceeded via the alkenylborane **88** and 4-hydroxyphenylcyclohexyl intermediates **90** and **92** shown in Schemes 9 and 10. This methodology was also employed as an alternative in the synthesis of the unsubstituted phenyl compound **30** and its pyrazine acid analogue **37**.

Spirocyclic acetic acid and tetrazole derivatives²³ having a 1,4-*trans* relationship between the acidic group and the direct aryl attachment on the cyclohexane ring were prepared by the annulation method shown in Schemes 11 and 12.

Analogous cyclohexanecarboxylic acids, with both *cis* and *trans* geometries, were obtained as described in Scheme 13.

Tetrazole analogue **82** was prepared by standard methodology from intermediate **110** (Scheme 14)

Similar boronation and coupling protocols (Scheme 15) gave access to the bicyclooctane acids **83** and **84**.

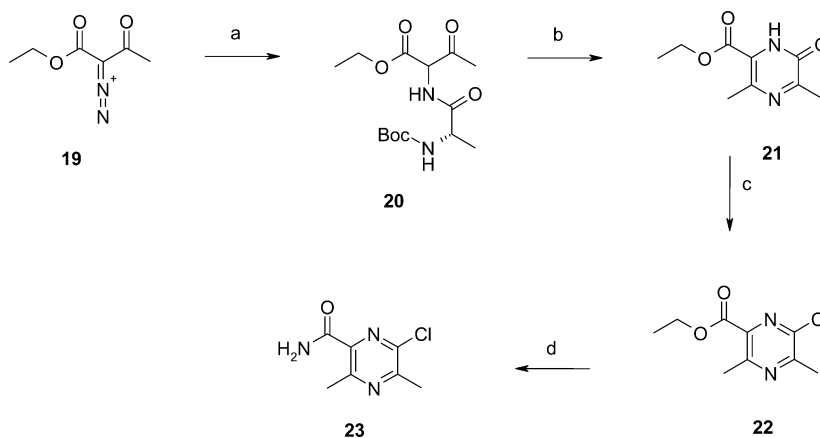
Tetrazole derivative **85** was obtained via the boronate intermediate **117** (Scheme 16).

The acylglucuronide derivative **120** of clinical candidate **30** was prepared following the method of Stachulski²⁸ (Scheme 17).

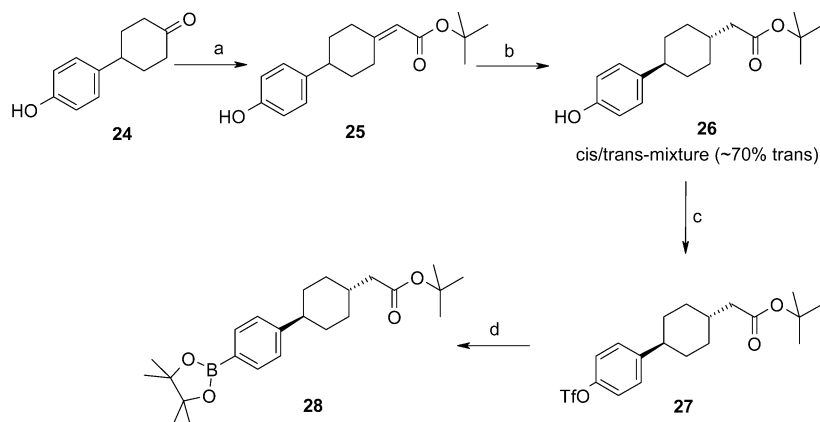
In summary herein is described the efficient syntheses of both mono- and disubstituted pyrazinecarboxamide structures coupled to various phenylcyclohexylacetic acid side chains, including substituted and spirocyclic variants, as well as those containing a carboxylic acid bioisostere replacing the acetic acid moiety.

RESULTS AND DISCUSSION

Compounds **12** and **13** (Table 1) were the first two analogues synthesized within the pyrazinecarboxamide series. Although modest in potency, they were on a par in terms of ligand lipophilicity efficiency (LLE) with the best oxadiazoles¹⁴ and achieved high selectivity over ACAT1 (Table 6). Furthermore, the compounds displayed excellent physicochemical properties as well as

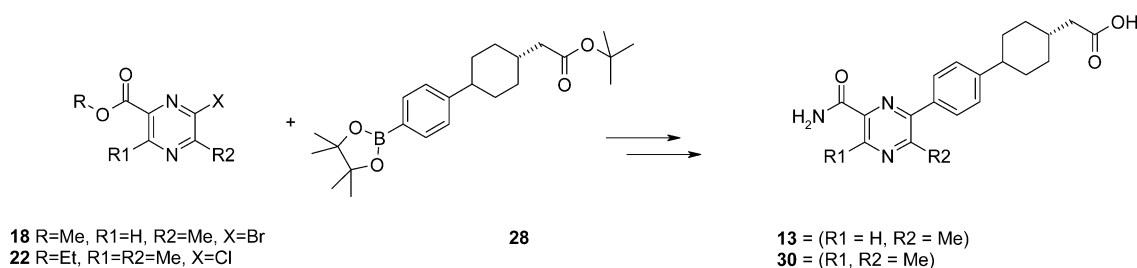
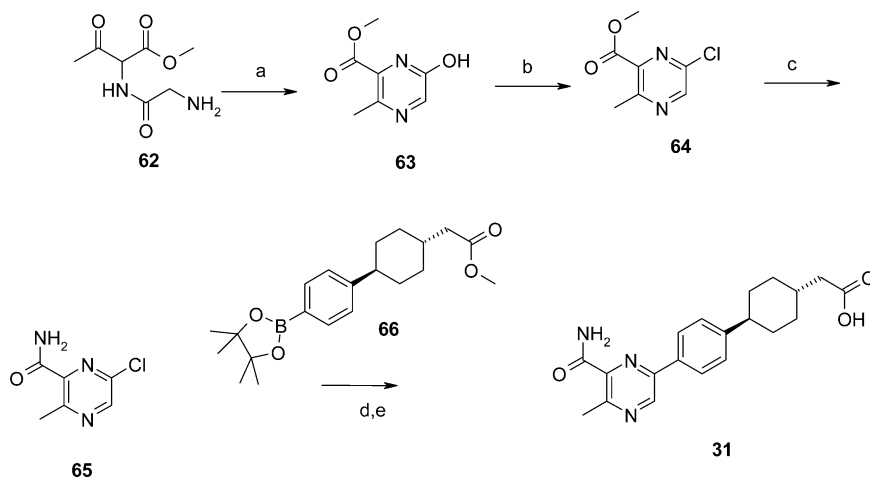
Scheme 4^a

^aReagents and conditions: (a) Rh₂Oct₄, toluene, 80 °C, Boc-Ala-NH₂; (b) TFA, DCE, reflux, 4 h; (c) POCl₃, BuCN, 150 °C, 10 min, microwave; (d) NH₃/MeOH.

Scheme 5^a

^aReagents and conditions: (a) NaH, *tert*-butyl (dimethoxyphosphoryl)acetate, THF, rt, overnight; (b) Pd/C, H₂, EtOAc, 5 bar, 3 h; (c) TFAA, pyridine, DCM, 0 °C, 30 min; (d) pinacolborane, Et₃N, Pd(dppf)Cl₂·DCM, reflux, 7 h.

Scheme 6

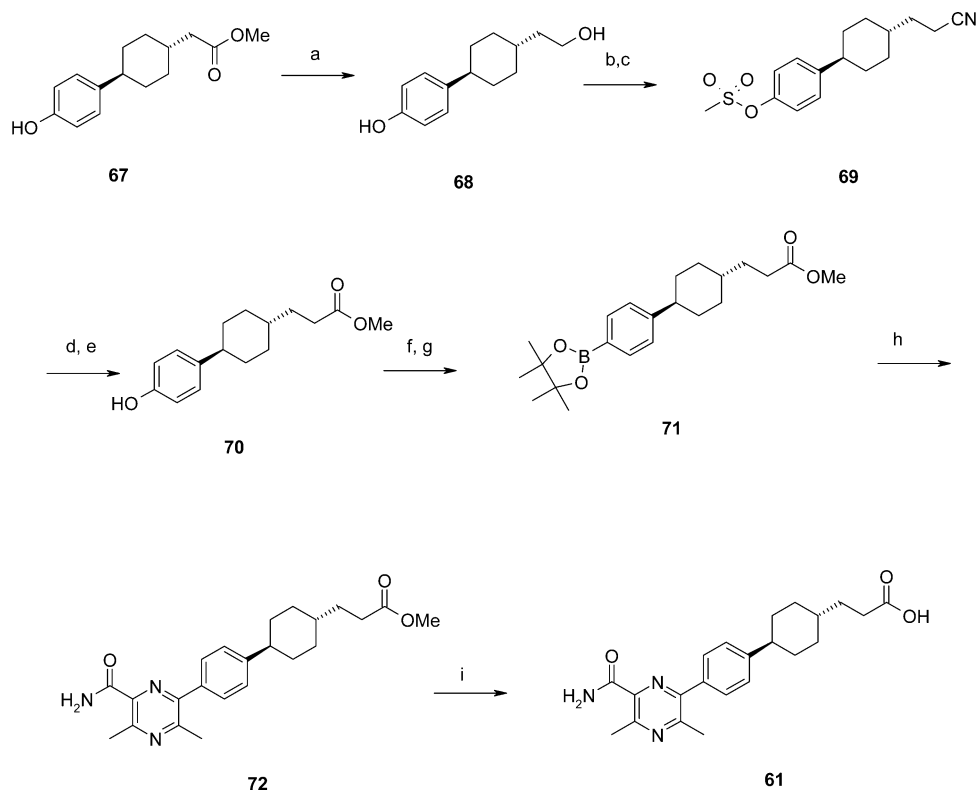
Scheme 7^a

^aReagents and conditions: (a) pyridine, 60 °C; (b) POCl₃, 90 °C; (c) 7 M NH₃ in MeOH, rt; (d) Pd(dppf)Cl₂·DCM, K₃PO₄, DME, EtOH, H₂O, 80 °C; (e) KOH, *t*-BuOH, 45 °C.

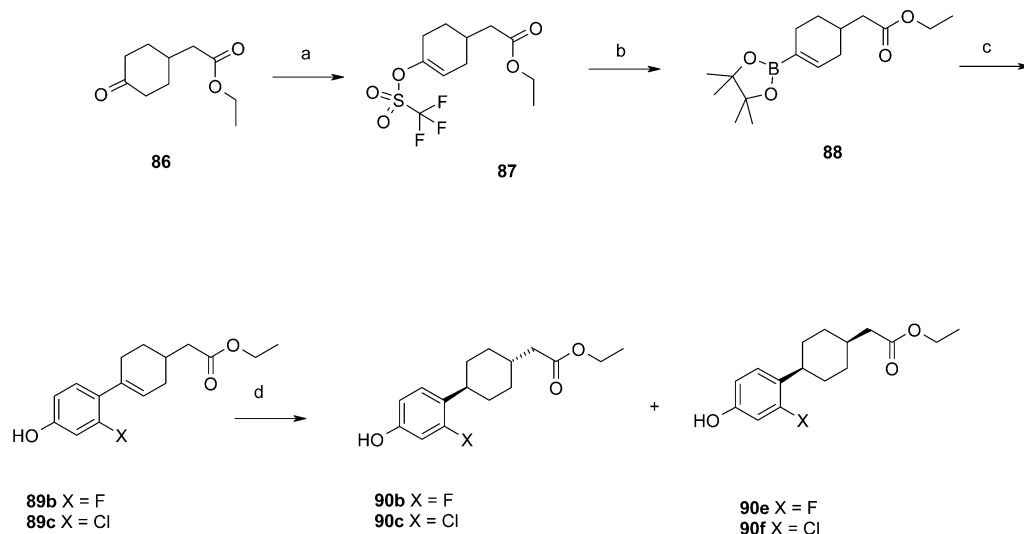
good DMPK properties (for 13) as described in Table 6. On the basis of these encouraging data, compounds 12 and 13 were selected as the starting point for a program to explore the structure–activity relationship within this series with the aim of improving potency while keeping good physicochemical and DMPK properties.

Removing a methyl group from 13 to give 29 or adding a second to give 30 (Table 1) gave significant shifts in potency, discussed further in the next section. Substitution of the left-hand side primary amide (Table 1, compounds 32–35) resulted in loss of potency, indicating the importance of both primary amide hydrogens for DGAT1 inhibition. Replacement of the primary

amide with a carboxylic acid, primary amine, amidine, or cyanoamide (36–40) was not tolerated. Thioamide 41 was the only attempted variation with retained potency in this part of the molecule, consistent with the supposition that the H-bond donor and acceptor are simultaneous requirements and must be presented to the DGAT1 protein syn to each other. Thioamide 41 displayed reduced lipophilicity ligand efficiency (LLE, Table 1) and reduced selectivity over ACAT1 (IC₅₀ = 16 μM) compared to 13. Thus, apart from generating interesting SAR information, thioamide 41 was not regarded as delivering any benefits over the corresponding amide 13.

Scheme 8^a

^aReagents and conditions: (a) 1 M LiAlH₄, THF, 0 °C; (b) MsCl, Et₃N, DCM; (c) NaCN, DMF, 80 °C; (d) NaOH, 1,2-propanediol, 140 °C; (e) MeOH, H₂SO₄; (f) TFAA, Et₃N, DCM; (g) pinacolborane, Pd(dppf)Cl₂·DCM, dppf, KOAc, dioxane, 85 °C; (h) 23, Pd(dtbpf)Cl₂, K₂CO₃, MeCN, 80 °C; (i) KOH, *t*-BuOH, 40 °C.

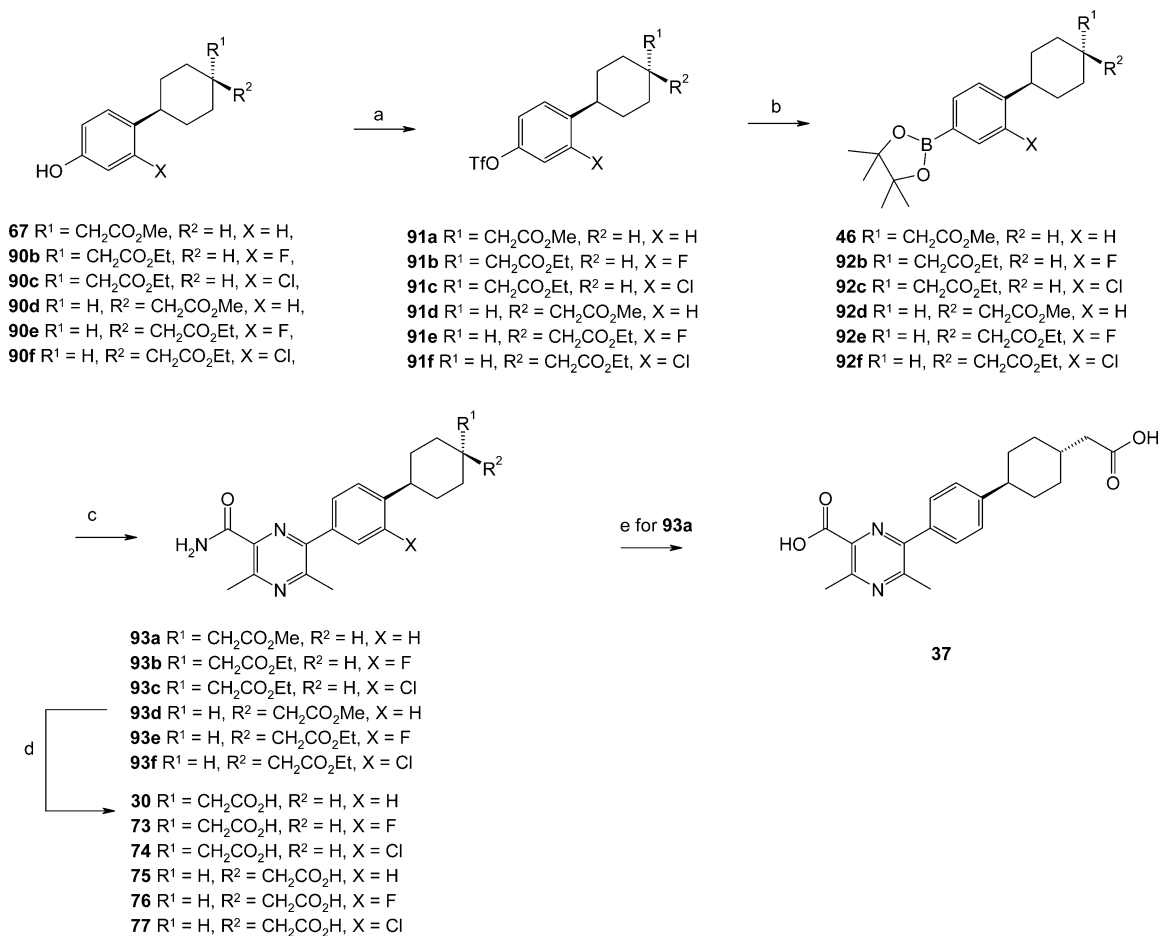
Scheme 9^a

^aReagents and conditions: (a) TFAA, 2,6-di-*tert*-butyl-4-methylpyridine, DCM, rt; (b) pinacolborane, KOAc, dppf, Pd(dppf)Cl₂·DCM, dioxane, 80 °C; (c) 4-bromo-3-fluorophenol or 4-bromo-3-chlorophenol, K₂CO₃, Pd(dppf)Cl₂·DCM, DMF, 100 °C; (d) 10% Pd/C, H₂, EtOH, rt.

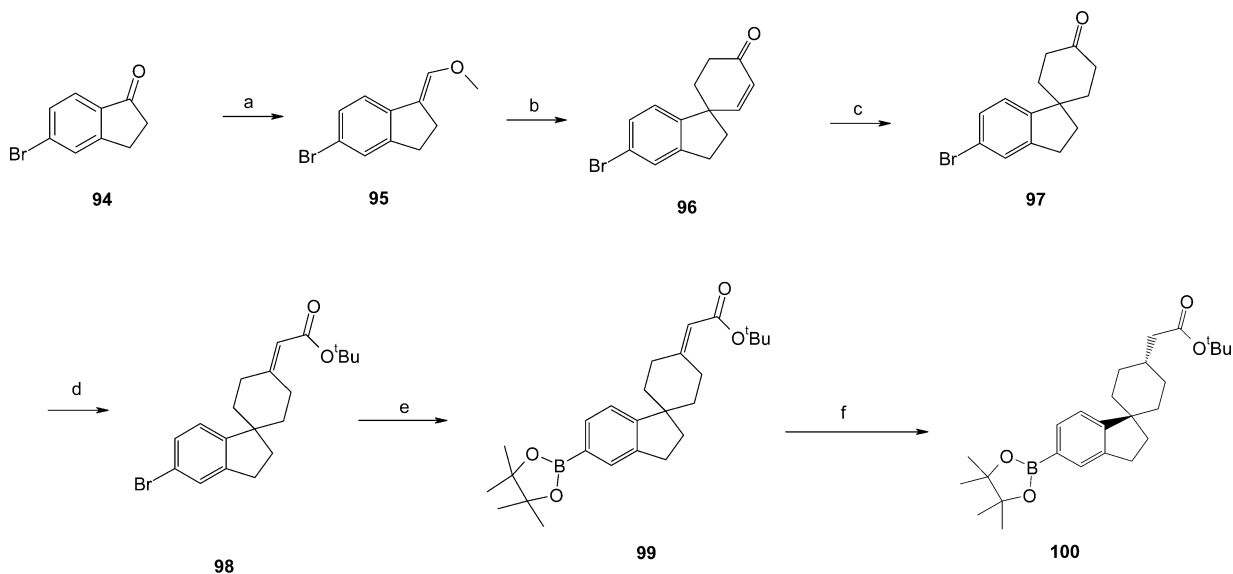
Pyridine analogues **42–44** (Table 2) show that both of the pyrazine nitrogens are important for DGAT1 inhibition.

As a next step we turned to investigate further the SAR for substituents on the pyrazine ring. The results from this investigation (Table 3) showed that for both R1 and R2 only small substituents were beneficial, particularly for R2, and methyl in both R1 and R2 (**30**) was the best of the combinations tried. Ethyl

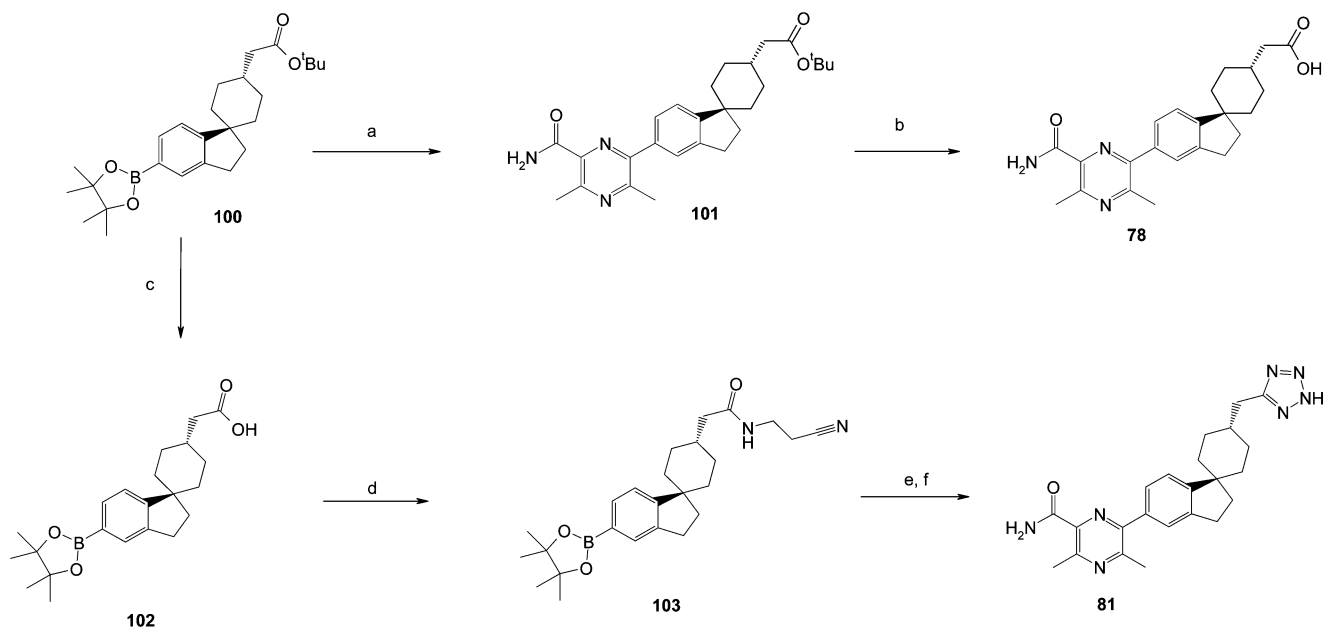
instead of methyl was not tolerated for R2 (**50**) and resulted in ~20-fold reduced potency at R1 (**46**). Addition of the methyl group in R1 turned out to be very successful, giving a 4-fold boost in potency for **30** compared to **13**. The added lipophilicity contribution from the R1 methyl was also seen to give a benefit on permeability and cell potency, without compromising the good physicochemical properties (Table 6). The R1 amino

Scheme 10^a

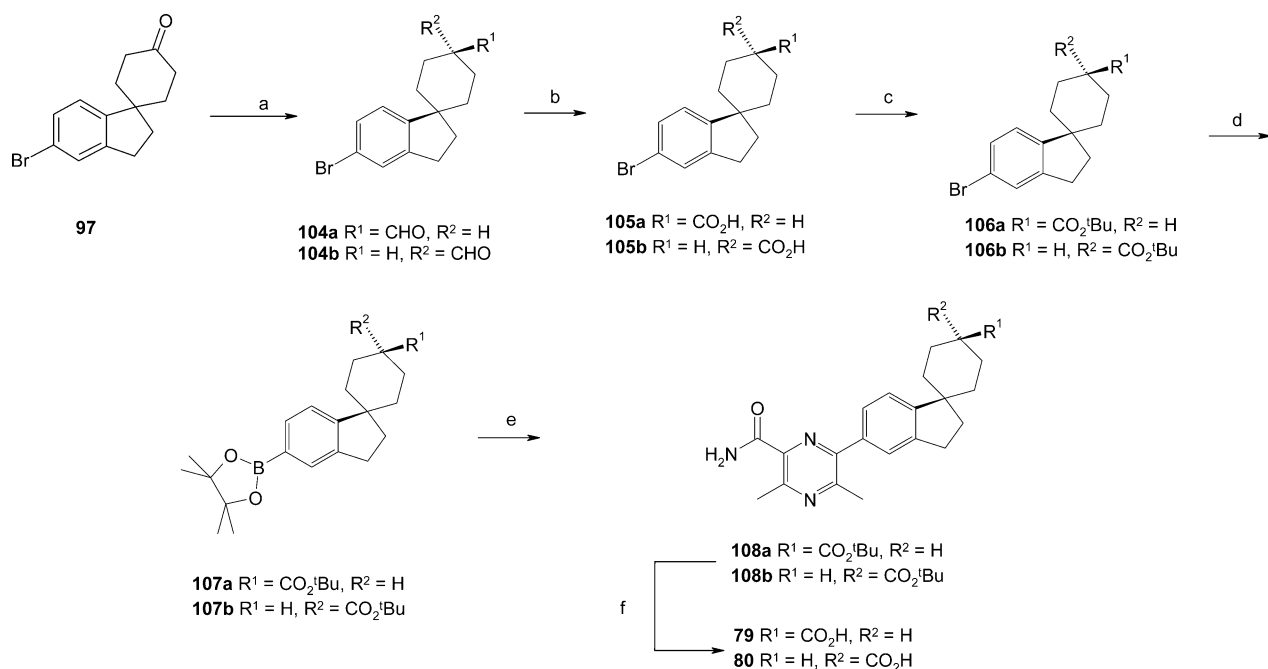
^aReagents and conditions: (a) TFAA, Et₃N, DCM, 0 °C; (b) pinacolborane, KOAc, dppf, Pd(dppf)Cl₂·DCM, dioxane, 80 °C; (c) **23**, K₃PO₄, Pd(dppf)Cl₂·DCM, DME, EtOH, H₂O, 80 °C; (d) KOH, *t*-BuOH, 40 °C; (e) 6 M HCl, dioxane, 100 °C.

Scheme 11^a

^aReagents and conditions: (a) (methoxymethyl)triphenylphosphonium chloride, KO-*t*-Bu, dioxane, rt; (b) methyl vinyl ketone, TsOH, toluene, 100 °C, 6 h; (c) 10% Pd/C, AcOH, H₂, rt; (d) *tert*-butyl diethylphosphonoacetate, NaH, THF, rt; (e) pinacolborane, KOAc, dppf, Pd(dppf)Cl₂·DCM, dioxane, 80 °C; (f) 10% Pd/C, THF, H₂, rt.

Scheme 12^a

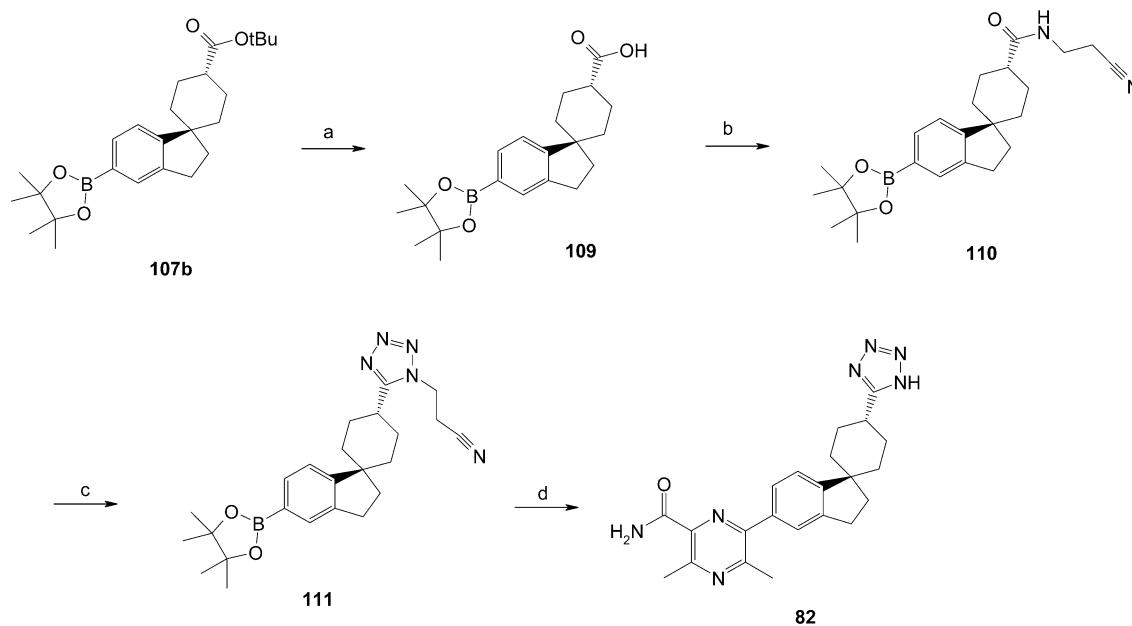
^aReagents and conditions: (a) **23**, K₂CO₃, Pd(dtbpf)Cl₂, MeCN, 80 °C; (b) TFA, DCM, rt; (c) TFA, DCM 0 °C; (d) 3-aminopropionitrile, PyBroP, DIPEA, DCM, rt; (e) TMSN₃, PPh₃, DIAD, THF, rt; (f) **23**, K₃PO₄, Pd(dppf)Cl₂·DCM, DME, EtOH, H₂O, 80 °C.

Scheme 13^a

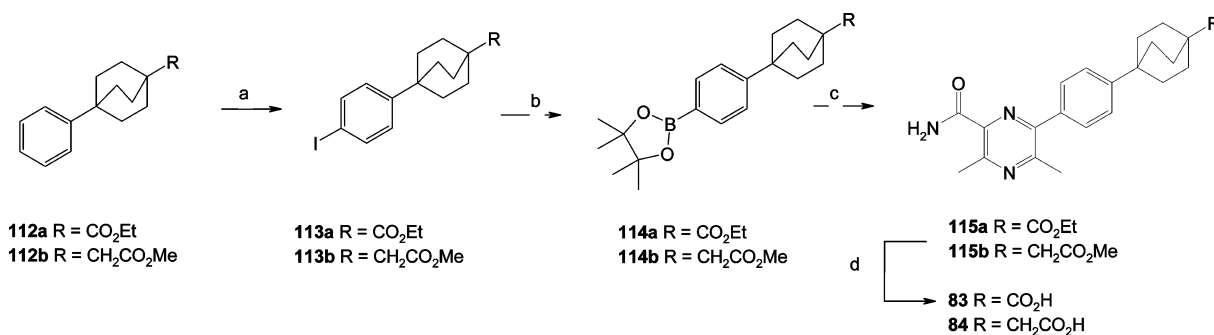
^aReagents and conditions: (a) (methoxymethyl)triphenylphosphonium chloride, KO-*t*-Bu, dioxane, 70 °C, 16 h; (b) Oxone, DMF, rt; (c) (Boc)₂O, DMAP, *t*-BuOH, rt to 70 °C; (d) pinacolborane, Pd(dppf)Cl₂·DCM, dppf, KOAc, dioxane, °C; (e) **23**, Pd(dppf)Cl₂·DCM, K₃PO₄, DME (8 mL), EtOH, H₂O; (f) 4 M HCl in dioxane, rt.

substituent in **49** was an attempt to lock the conformation of the primary amide via an internal hydrogen bond. Compound **49**, however, was inactive, suggesting that the polar NH not involved in the H-bond to the carbonyl is not tolerated in a region in which the potent compound **2** has an acceptor (a pyrimidine N).

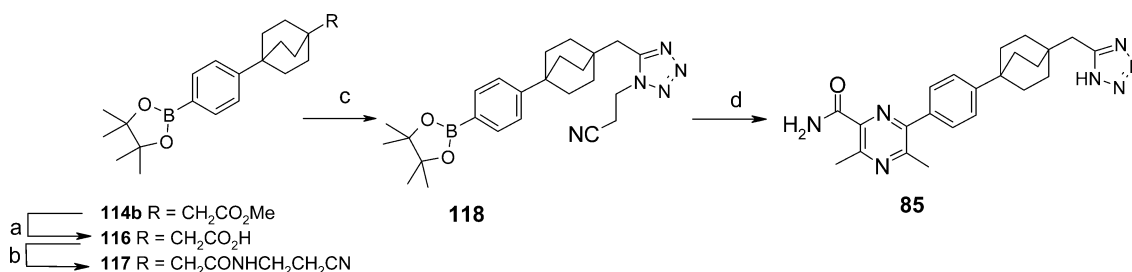
In contrast to the so far relatively steep SAR found for the left and middle parts of the molecules, variations to the right-hand side carboxylic acid were all found to result in highly potent compounds as outlined in Table 4. The 3,5-dimethylpyrazine group continued to deliver good potency in these analogues. The higher log *D* of the neutral alcohols (**53**, **54**)

Scheme 14^a

^aReagents and conditions: (a) TFA, DCM, 0 °C; (b) 3-aminopropionitrile, PyBroP, DIPEA, DCM, rt; (c) TMSN₃, PPh₃, DIAD, THF, rt; (d) 23, K₃PO₄, Pd(dppf)Cl₂, DME, EtOH, H₂O, 80 °C.

Scheme 15^a

^aReagents and conditions: (a) PhI(OCCF₃)₂, I₂, CHCl₃; (b) pinacolborane, Pd(dppf)Cl₂-DCM, KOAc, DMSO; (c) 23, Pd(dppf)Cl₂-DCM, K₃PO₄, DME, EtOH, H₂O; (d) KOH, *t*-BuOH, 45 °C.

Scheme 16^a

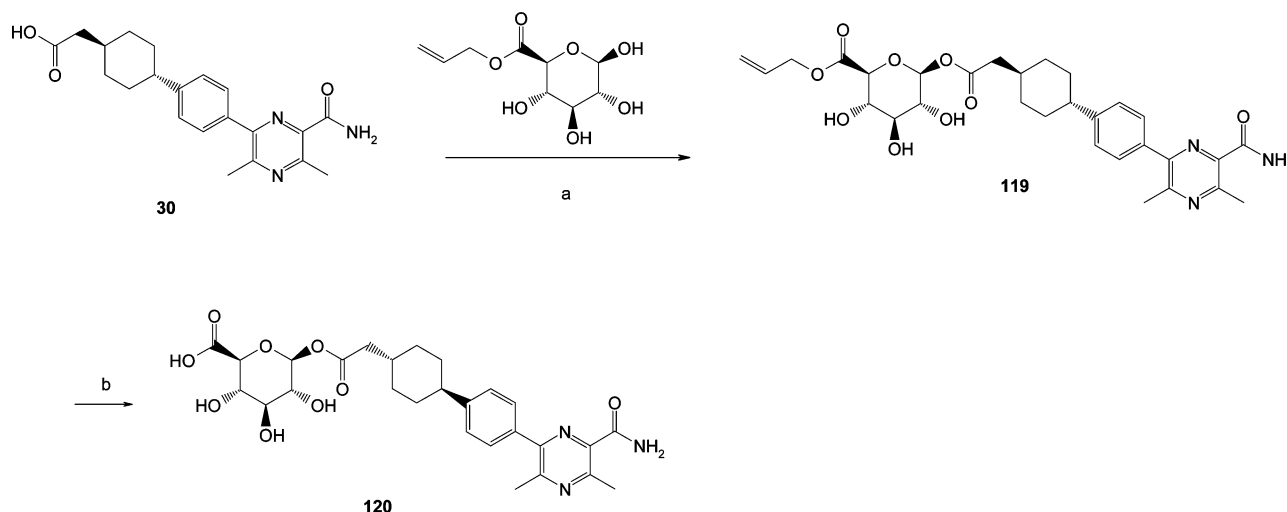
^aReagents and conditions: (a) NaOH, MeOH, H₂O, 120 °C, microwave; (b) 3-aminopropionitrile, PyBroP, DIPEA, DCM, rt; (c) TMSN₃, PPh₃, DIAD, THF, rt; (d) 23, Pd(dppf)Cl₂-DCM, K₃PO₄, DME, EtOH, H₂O, 80 °C.

and amides (55, 56), however, resulted in reduced aqueous solubility (Table 6).

Elongation with an amino acid as in 57 and 58 and introduction of carboxylic acid bioisosteres as the acylated sulfonamide 59 and tetrazole 60 all resulted in compounds with good

potency and good physicochemical properties (Table 6). Similar right-hand side SAR has been described for the Japan Tobacco/Tularic series.²³

Variation of the phenylcyclohexane core was next examined. Simple fluoro or chloro substitution ortho to the cyclohexyl

Scheme 17^a

^aReagents and conditions: (a) HATU, DABCO, MeCN, rt; (b) Pd(PPh₃)₄, pyrrolidine, THF, rt.

group²³ (compounds 73 and 74) maintained DGAT1 activity. 1,4-Cis substitution was investigated for a small number of analogues (75–77). Potency was maintained, but no advantage over the more readily accessible trans isomers was identified. Various spirocyclic analogues²³ (78–82) were investigated, seeking potency enhancement from a locked conformation between the phenyl and cyclohexyl rings. Although these proved to be some of the most potent compounds, their intrinsic higher lipophilicities led to no advantage in overall properties to offset their synthetic complexity. In a previous series of DGAT1 inhibitors we had utilized the bicyclooctane system as an alternative to cyclohexyl.³ This system maintained potency in the present series (compounds 83–85) but again with the disadvantage of increased lipophilicity.

Wider selectivity and physical and DMPK properties for representative compounds are given in Table 6. In general potency against ACAT1 was low, the good selectivity for DGAT1, which was a prerequisite of the program, thus being achieved. Erosion of the margin to less than 100-fold for the spirocyclic compound 78 precluded its further development. Aqueous solubility was generally good as might be expected from carboxylic acids of relatively low lipophilicity. This was combined with good permeability for the simple carboxylic acids, as measured in the Caco-2 or MDCK assay, which was reassuring because low permeability can be an issue for compounds that have log *D* < 1.7 with molecular weight in the 350–400 range.²⁰ Low intrinsic clearance was seen generally with the acids in Table 6. These properties combined to give very good rat PK profiles with long oral half-lives and high bioavailability seen across a range of core structures. The short half-life of primary alcohol 53 presumably reflects the metabolic instability of this functionality. The elements in Table 6 were considered alongside synthetic accessibility, and compound 30 was chosen for extensive *in vitro* and *in vivo* profiling as a potential candidate drug. Full data are presented in Table 7.

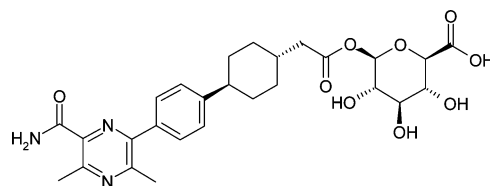
Compound 30 showed similar inhibitory potency against recombinant human protein and against that expressed in human liver microsomes (Table 7). Potency was found to be significantly higher when assessed in human adipose tissue explants and in an intestinal cell line (HuTu80). Little difference in DGAT1 activity was encountered across species. No activity was seen against human DGAT2 and ACAT2. The compound was

free of activity against the hERG encoded ion channel and against a panel of common CYP P450 enzymes. In a panel of 339 *in vitro* radioligand binding and enzyme assays covering a diverse range of enzymes, receptors, ion channels, and transporters, compound 30 showed inhibition of acyl-CoA:cholesterol acetyltransferase (79% at 10 μM), fatty acid amide hydrolase (IC₅₀ = 3.7 μM), muscarinic M2 receptor (IC₅₀ = 80.5 μM), and phosphodiesterase PDE10A1 (IC₅₀ = 5.5 μM). Plasma protein binding was relatively consistent across species.

This compound also proved to have excellent pharmaceutical properties with high solubility and permeability from a crystalline nonhygroscopic single polymorph. No issues were encountered with chemical or light stability.

Compound 30 pharmacokinetics were determined in mice, rats, and dogs (Table 8). Low metabolic clearance and volume of distribution were observed in each species with good to excellent bioavailability. These data in combination with the very low turnover seen in human hepatocytes predicted an attractive PK profile in man.

The most significant metabolite identified in human, rat, and dog hepatocytes was the acyl glucuronide 120. It is believed that in some circumstances the initially formed 1β-isomer of an acyl glucuronide metabolite can directly lead to drug–protein covalent conjugates through acylation, while the 2- and 4-*O*-acyl rearrangement products can give rise to adducts through Schiff base formation with protein amino groups.²⁸ The *in vitro* stability of acyl glucuronide 120 was assessed in pH 7.8 buffer: no measurable degradation or acyl migration was observed over 45 min, giving confidence that this metabolite would be unlikely to give rise to safety issues in man.



120

The pharmacodynamic effects of compound 30 were determined in the rat oral lipid tolerance test (OLTT) and the

Table 1. Initial Pyrazine Primary Amide and N-Substituted Amide SAR

| Compound | R | n | hDGAT1 IC ₅₀ (μM) ^a | LogD ^b | LLE |
|----------|---|---|---|-------------------|-------|
| 12 | | 0 | 1.1 | 0.22 | 5.7 |
| 13 | | 1 | 0.31 | 0.3 | 6.2 |
| 29 | | 1 | 1.9 | <0.1 | > 5.6 |
| 30 | | 1 | 0.08 | 0.9 ^c | 6.2 |
| 31 | | 1 | 0.59 | 1.0 ^c | 5.2 |
| 32 | | 1 | inactive | 0.9 | |
| 33 | | 1 | inactive | 0.7 | |
| 34 | | 1 | inactive | 2.7 | |
| 35 | | 1 | Inactive | 0.7 | |
| 36 | | 1 | inactive | <0 | |
| 37 | | 1 | inactive | NT | |
| 38 | | 1 | inactive | <0 | |
| 39 | | 1 | > 33 | <0 | |
| 40 | | 1 | inactive | 1.2 | |
| 41 | | 1 | 0.11 | 1.8 | 5.2 |

^aMean values from a minimum of three experiments. ^bChromatographic log *D*, pH 7.4, unless otherwise indicated: Waters ACQUITY UPLC BEH C18 1.7 μm, 50 mm × 2.1 mm column; mobile phase 10 mM ammonium acetate in CH₃CN/H₂O, 95/5 to 5/95 gradient elution; log *D* calculated from retention time vs standard curve. ^cOctanol/water partitioning, pH 7.4.

Table 2. Pyrazine Replaced by Pyridines

| Compound | R | hDGAT1 (% inhibition at 10 μM) ^a | LogD ^b | LLE |
|----------|---|---|-------------------|------|
| 42 | | 60 | 0 | <5.3 |
| 43 | | 28 | 0.8 | <4.2 |
| 44 | | 41 | 1.3 | <3.7 |

^aMean values from a minimum of three experiments. ^bChromatographic log *D*, as in Table 1.

Table 3. Pyrazine Substitution

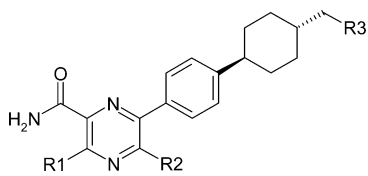
| compd | R1 | R2 | hDGAT1 IC ₅₀ (μM) ^a | log <i>D</i> ^c | LLE |
|-------|------------------|--------------|---|---------------------------|------|
| 30 | Me | Me | 0.08 | 0.9 ^d | 6.2 |
| 45 | CHF ₂ | Me | 0.41 ^b | 1.4 | 5.0 |
| 46 | Et | Me | 1.8 | 1.5 | 4.2 |
| 47 | <i>i</i> -Pr | Me | >10 | 2.6 | <2.4 |
| 48 | Ph | Me | >10 | 2.0 | <3.1 |
| 49 | NH ₂ | H | >10 | 0.5 | <4.5 |
| 50 | Me | Et | >9.1 | 1.7 | <3.3 |
| 51 | Me | <i>i</i> -Pr | >10 | 2.6 | <2.4 |
| 52 | Me | Ph | >10 | 2.5 | <2.5 |

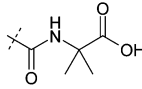
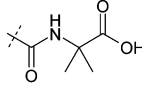
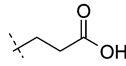
^aMean values from a minimum of three experiments. ^bMean value from two experiments. ^cChromatographic log *D* method, as in Table 1. ^dOctanol/water partitioning, pH 7.4.

rat TAG synthesis test. Figure 1 shows the relationship between plasma triglycerides and free compound levels in plasma for compound **30** in the rat OLTT assay. Compound **30** was able to inhibit appearance of TAG in plasma following the lipid challenge in an exposure dependent manner. A direct response PK/PD model (E_{\max} sigmoidal model) was used to successfully fit the PK/PD data showing a clear correlation between free compound levels in plasma and an effect in the OLTT. PK/PD parameters for the model fit are shown in Table 9. The in vivo IC₅₀ (0.042 μM) is in very good agreement with the in vitro one (0.080 μM), suggesting that free concentrations in plasma are a good surrogate for pharmacological active drug levels in the gut cells in the OLTT assay.

Figure 2 shows the relationship between adipose TAG synthesis (expressed as TAG/DAG ratio in adipose tissue) and free compound levels in plasma for compound **30** in the rat.

Table 4. Carboxylic Acid Replacements and Variations



| Compound | R1 | R2 | R3 | hDGAT1 (μM) ^a | LogD ^b | LLE |
|----------|----|----|---|--|-------------------|------|
| 53 | Me | Me |  | 0.69 | 3.1 | 3.1 |
| 54 | H | H |  | 1.2 | 2.3 | 3.6 |
| 55 | Me | Me |  | 0.52 | 1.7 | 4.6 |
| 56 | H | H |  | 1.9 | 0.9 | 4.8 |
| 57 | Me | Me |  | 0.11 | 0.7 | 6.3 |
| 58 | H | H |  | 1.1 | <0.1 | >5.9 |
| 59 | Me | Me |  | 0.10 | 0.9 | 6.1 |
| 60 | Me | Me |  | 0.06 | 0.8 | 6.5 |
| 61 | Me | Me |  | 0.12 | 1.6 ^c | 5.3 |

^aIC₅₀: mean values from a minimum of three experiments. ^bChromatographic method as in Table 1. ^cOctanol/water partitioning as in Table 1.

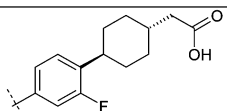
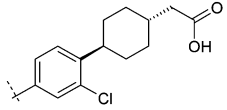
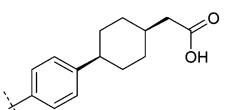
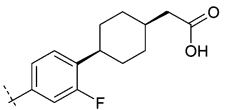
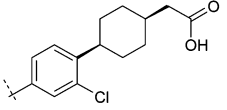
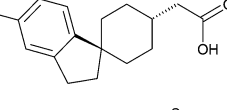
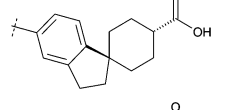
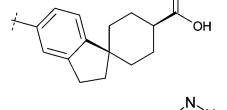
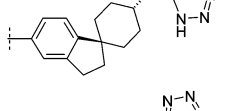
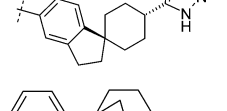
Compound **30** was able to reduce the formation of TAG in adipose tissue (measured as TAG/DAG ratio) in an exposure dependent manner. A direct response PK/PD model (E_{max} model) was used to successfully fit the PK/PD data showing a clear correlation between free compound levels in plasma and an effect in the adipose TAG/DAG ratio. PK/PD parameters for the model fit are shown in Table 10. The in vivo IC₅₀ (0.132 μM) in the adipose tissue assay also is in very good agreement with the in vitro IC₅₀ (0.080 μM), showing once again that free plasma concentrations are a good surrogate for pharmacological active drug levels in the adipose tissue cells in the TAG synthesis assay. In addition compound **30** was shown to have beneficial effects in several preclinical metabolic disease models (e.g., enhanced GLP-1 secretion, delayed gastric emptying, reduced food intake,

improved insulin sensitivity, reduced atherosclerosis), and these will be described in detail elsewhere.

On the basis of the attractive profile described above Compound **30** was selected as a clinical candidate drug. Figure 3 gives the rising dose PK profile from human volunteer studies.

At all dose levels studied, compound **30** was rapidly absorbed with the maximal plasma concentration reached within 1 h with exposure increasing proportionally with dose (Figure 3). The geometric mean terminal half-life estimated at all dose levels ranged between 9 and 14 h. These data are consistent with the preclinical DMPK and physicochemical data presented above. Pharmacodynamic data, to be published elsewhere, indicated 5 mg u.i.d. as an effective dose for lowering serum triglyceride following a standardized mixed meal.

Table 5. Phenylcyclohexylacetic Acid Variations

| Compound | R | hDGAT1 (μM) ^a | LogD ^b | LLE |
|----------|---|--|-------------------|-----|
| 73 |  | 0.06 | 1.3 | 6.0 |
| 74 |  | 0.03 | 1.8 | 5.7 |
| 75 |  | 0.43 | ND | ND |
| 76 |  | 0.12 | 1.2 | 5.7 |
| 77 |  | 0.07 | 1.5 | 6.1 |
| 78 |  | 0.03 | 1.5 | 6.1 |
| 79 |  | 0.17 | 1.2 | 5.6 |
| 80 |  | 0.24 | 1.3 | 5.3 |
| 81 |  | 0.03 | 2.0 | 5.5 |
| 82 |  | 0.12 | 1.4 | 5.5 |
| 83 |  | 0.08 | 1.6 | 5.5 |
| 84 |  | 0.20 | 1.3 | 5.4 |
| 85 |  | 0.04 | ND | ND |

^aIC₅₀: mean values from a minimum of three experiments. ^bOctanol/water partitioning as in Table 1.

Table 6. Wider Selectivity and Physical and DMPK Properties for Representative Compounds

| compd | MW | DGAT1 IC ₅₀ (μM) | ACAT1 IC ₅₀ (μM) | solubility, ^a pH 7.4 (μM) | human plasma protein binding ^b (% free) | rat hepatocyte intrinsic clearance ^c (μL/min)/10 ⁶ cells | permeability <i>P</i> _{app} ^d (×10 ⁻⁸ cm/s) | rat oral half-life ^f (h) | rat bioavailability (%) |
|-------|-----|--------------------------------|--------------------------------|---|---|--|--|---|-------------------------------|
| 12 | 339 | 1.1 | 79 | 1200 | NT | 72 | NT | NT | NT |
| 13 | 353 | 0.34 | >33 | >100 | 5.7 | <6 | 35 ^e | 5.7 | 80 |
| 29 | 339 | 1.9 | >100 | NT | 3.5 | NT | 29 ^e | 11 | 62 |
| 30 | 367 | 0.08 | 34 | 700 | 4.7 | <2 | 12 | 14 ^g | 93 |
| 53 | 353 | 0.69 | 75 | 4 | 3.0 | NT | 58 ^e | 0.26 | 3 |
| 54 | 325 | 1.2 | NT | 3 | 2.8 | 36 | 38 ^e | NT | NT |
| 55 | 366 | 0.52 | 25 | NT | 13 | 77 | 18 | NT | NT |
| 56 | 338 | 1.9 | NT | <1 | NT | NT | 13 ^e | NT | NT |
| 57 | 452 | 0.11 | NT | 86 | 7.8 | NT | 0.71 ^e | 1.9 | 19 |
| 58 | 424 | 1.1 | NT | >100 | NT | <2 | NT | NT | NT |
| 59 | 444 | 0.10 | NT | 100 | 11 | 17 | 2.0 ^e | 0.43 | 32 |
| 60 | 391 | 0.06 | 44 | 270 | 0.9 | <2 | 3.7 | 9.0 ^g | 18 |
| 78 | 393 | 0.03 | 2.4 | 562 | 1.3 | <2 | 12 | 7.5 ^g | 65 |
| 83 | 393 | 0.08 | 15 | 113 | 0.6 | <2 | 13 | 7.3 ^g | 55 |

^aSolubility determined in 0.1 M phosphate buffer, pH 7.4, at 25 °C for 24 h. ^bPPB was assessed by equilibrium dialysis in the appropriate species plasma at 37 °C. Free and bound concentrations were quantified by LC–UVMS. ^cCompounds were incubated at 1 μM with suspended rat hepatocytes at 1 × 10⁶ cells/mL, and intrinsic clearance was calculated from rate of disappearance of parent. ^dPermeability measured in MDCK cells in the A to B direction, pH 7.4. ^ePermeability measured in Caco2 cells in the A to B direction, pH 7.4. ^fOral dosing in female Sprague–Dawley rats at 4.0 μM/kg in DMA/tetraethylene glycol/water, 1:1:1, solution. ^gOral dosing in male Han–Wistar rats at 2.54–5.4 μM/kg in water/(5% DMSO/95% hydroxypropyl β-cyclodextrin), 25% w/v.

Table 7. Full Potency, Selectivity, DMPK, and Physical Properties for Compound 30

| human DGAT1 recombinant ^a | human DGAT1 liver microsome ^{a,b} | human adipose tissue ^{a,b} | human intestinal cell HuTu80 ^a | human DGAT2 ^a | human ACAT1 ^a | human ACAT2 ^a |
|--|--|--|--|--|--|--|
| 0.08 | 0.07 | 0.01 | 0.01 | >300 | 34 | >10 |
| rat DGAT1 liver microsome ^{a,b} | rat adipose tissue ^{a,b} | mouse DGAT1 liver microsome ^{a,b} | dog DGAT1 liver microsome ^{a,b} | human plasma protein binding ^c | rat plasma protein binding ^c | mouse plasma protein binding ^c |
| 0.15 | 0.09 | 0.10 | 0.06 | 5.5 | 3 | 10 |
| dog plasma protein binding ^c | hERG ^a | CYP P450 ^a | crystalline solubility, pH 7.4 (μM) | chemical stability (25 °C across pH 1–10) | photostability Hannau sun test | |
| 6 | >32 | >30 vs 1A2, 2C9, 2C19, 2D6, 3A4 | 700 | <i>t</i> _{1/2} > 100 days | <i>t</i> _{1/2} = 7.6 h | |
| human hepatocyte CL _{int} (μL/min)/10 ⁶ cells | mouse hepatocyte CL _{int} (μL/min)/10 ⁶ cells | rat hepatocyte CL _{int} (μL/min)/10 ⁶ cells | dog hepatocyte CL _{int} (μL/min)/10 ⁶ cells | permeability Caco-2 (×10 ⁻⁶ cm·s ⁻¹) | permeability MDCK (×10 ⁻⁶ cm·s ⁻¹) | |
| <2 | 7.3 | <2 | 5.5 | 11 | 12 | |

^aIC₅₀, μM. ^bSee Experimental Section for assay details. ^c% free.

Table 8. PK Parameters for Compound 30

| | mouse ^a | rat ^b | dog ^c |
|-------------------------------|--------------------|------------------|------------------|
| clearance ((mL/min)/kg) | 0.77 | 0.50 | 1.2 |
| volume of distribution (L/kg) | 0.9 | 0.35 | 1.0 |
| half-life (h) | 13 | 14 | 11 |
| bioavailability (%) | >100 | 93 | ~100 |

^aOral dosing at 8.16 μM/kg as an aqueous suspension with hydroxypropyl methylcellulose/Tween, iv dosing as a solution at 5.4 μM/kg in male C57 BL/6 mice. ^bOral dosing as a solution at 5.4 μM/kg, iv dosing as a solution at 2.7 μM/kg in male Han–Wistar rats. ^cOral dosing at 27.2 μM/kg as a suspension (hydroxypropyl β-cyclodextrin/Tween), iv dosing at 1.4 μM/kg as a solution in Beagle dogs. All solutions in water/(5% DMSO/95% hydroxypropyl β-cyclodextrin), 25% w/v.

CONCLUSION

The herein described rational design and optimization of a series of compounds based on a pyrazinecarboxamide core structure culminated in the identification of the clinical candidate drug compound 30 (AZD7687). This compound fulfilled the design objectives set at the start of the program, as it showed high selectivity for DGAT1 over ACAT1 and had very good physicochemical and preclinical DMPK properties that translated into a

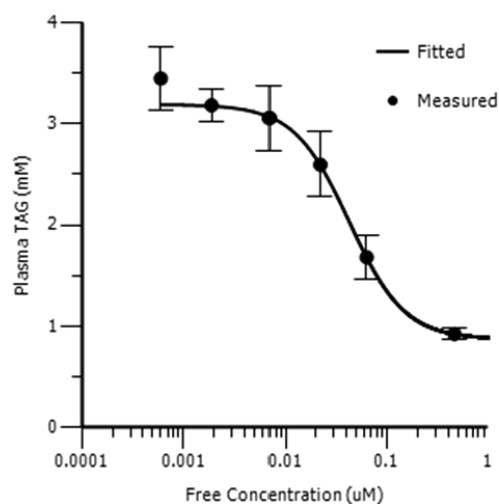
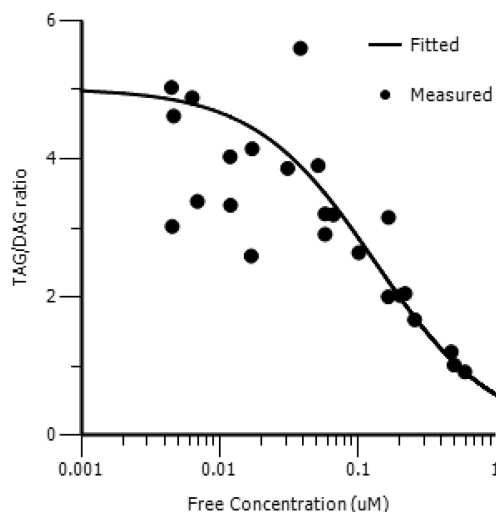


Figure 1. PK/PD analysis of rat OLTT (plasma triglycerides (mean ± SEM) vs free compound concentrations in plasma) for compound 30. A direct response (*E*_{max} sigmoidal) model was used to fit the PK/PD data.

desirable clinical PK profile consistent with a low efficacious dose in man.

Table 9. PK/PD Parameters for Model Fit for Compound 30 in the Rat OLTT

| parameter | $E = E_0 - [(I_{\max}C^{\gamma}) / (IC_{50}^{\gamma} + C^{\gamma})]$ | | |
|------------|--|---------------|-----------|
| | estimate | units | Stderr, % |
| IC_{50} | 0.042 | μM | 10 |
| γ | 1.6 | | 19 |
| E_0 | 3.2 | mM | 2.7 |
| I_{\max} | 2.3 | mM | 5.1 |

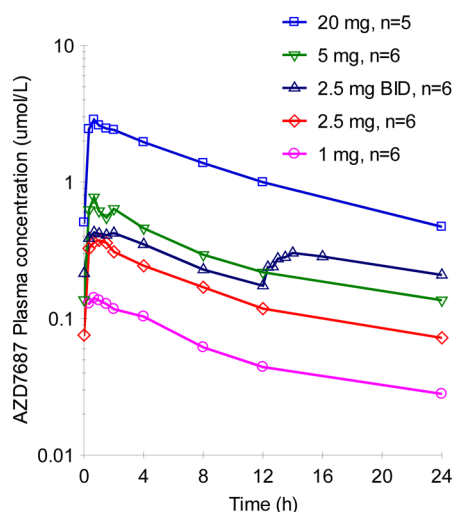
**Figure 2.** PK/PD analysis of rat adipose TAG synthesis assay (adipose tissue TAG/DAG ratio vs free compound concentrations in plasma) for compound 30. A direct response (E_{\max} model) was used to fit the PK/PD data.**Table 10. PK/PD Parameters for Model Fit for Compound 30 in the Rat Adipose TAG Synthesis Assay**

| parameter | $E = E_0 \{1 - [C / (IC_{50} + C)]\}$ | | |
|-----------|---------------------------------------|---------------|-----------|
| | estimate | units | Stderr, % |
| IC_{50} | 0.132 | μM | 13 |
| E_0 | 5.0 | | 4.9 |

EXPERIMENTAL SECTION

All solvents and chemicals used were reagent grade. Anhydrous solvents tetrahydrofuran (THF) and dimethoxyethane (DME) were purchased from Aldrich and used as such. Flash column chromatography was carried out using prepacked silica cartridges (from 4 to 330 g) from Redisp, Biotage, or Crawford and with elution using an Isco Companion system. Purity and characterization of compounds were established by a combination of liquid chromatography–mass spectrometry (LC–MS), gas chromatography–mass spectrometry (GC–MS), and NMR analytical techniques. ^1H NMR spectra were recorded on Bruker Avance DPX400 (400 MHz), DPX300 (300 MHz), and AV700 (700 MHz) instruments and were determined in CHCl_3 - d , $\text{DMSO}-d_6$, and $\text{MeOH}-d_4$ with trimethylsilane (TMS) (0.00 ppm) or solvent peaks as the internal reference. Chemical shifts are reported in ppm relative to solvent signal, and coupling constants (J) are reported in hertz (Hz). Splitting patterns are indicated as follows: s, singlet; d, doublet; t, triplet; m, multiplet; br, broad peak. Merck precoated thin layer chromatography (TLC) plates (silica gel 60 F_{254} , 0.25 mm, article 5715) were used for TLC analysis. Solutions were dried over anhydrous magnesium sulfate, and the solvent was removed by rotary evaporation under reduced pressure.

DGAT1, DGAT2, ACAT1, and ACAT2 in vitro assay protocols and measurement of triacylglycerol synthesis in HuTu 80 cells were as previously described.³ Oral lipid tolerance test (OLTT) and adipose

**Figure 3.** Mean plasma concentration from ascending doses of compound 30 in human volunteers.

triacylglycerol synthesis tests in the rat protocols were again as previously described.³

Human liver microsomes were purchased from the UK Human Tissue Bank. Rat, mouse, and dog microsomes were prepared from fresh liver according to the method described by Coleman.²⁹ DGAT activity was then assayed as previously described.³

For the adipose TAG synthesis assay, measurement of TAG and DAG synthesis in rat epididymal and human subcutaneous adipose tissue was performed ex vivo by measurement of ^{14}C palmitate incorporation into TAG and DAG, and this was used to obtain an index of DGAT1 activity.

The human adipose tissue samples were obtained from volunteers by needle biopsies of abdominal subcutaneous tissue following local anesthesia. This procedure was approved by the Regional Ethical Review Boards in Gothenburg and Umeå, respectively, and the South Cheshire Local Research Ethics Committee. Written informed consent was obtained from all subjects prior to initiation of any study-related procedures. The human adipose tissue biopsy was washed in PBS (Gibco, Paisley, U.K.). To remove excess medium and blood clots, the biopsy was put on a cell strainer with a paper napkin underneath. Whole rat epididymal fat pads were removed. Approximately 3×50 mg of adipose tissue from each species was placed into a 48-well tissue culture plate. The adipose tissue was incubated with 200 μL of DMEM (6 mM glucose, 5% FCS (Gibco, Paisley, U.K.), 0.5% penicillin/streptomycin (Gibco, Paisley, U.K.) containing compound dissolved in DMSO (0.1% final concentration) for 30 min at 37 $^{\circ}\text{C}$, 5% CO_2 . ^{14}C palmitic acid (2.5 $\mu\text{Ci}/\text{mL}$) and a mixture of sodium palmitate complexed to BSA (0.12 mM sodium palmitate, 0.03 mM BSA final concentration) were added to the wells and the samples incubated for a further 2 h for the human adipose tissue and 3 h for the rat adipose tissue at 37 $^{\circ}\text{C}$, 5% CO_2 . The culture medium was removed, and the biopsies were transferred to lysis matrix D tubes.

The lipids were extracted using the Folch extraction method. An amount of 1 mL of methanol plus ^3H -oleate (to account for losses during the extraction phase) was added to each sample. The tissue was homogenized (FastPrep), and the contents were transferred to glass Pyrex tubes. The lysis matrix D tubes were washed with 1 mL of methanol, and the contents were transferred to the glass Pyrex tubes. An amount of 4 mL of chloroform was added before the tubes were vortexed and incubated at 40 $^{\circ}\text{C}$ for 1 h. Then 1.2 mL of saline (0.73%) was added and the glass Pyrex tubes were vortexed and left in a fridge overnight to separate. The bottom solvent layer was transferred into a fresh tube and solvent was evaporated under a stream of nitrogen. The extract was solubilized in isohexane/acetic acid (99:1). Lipids were separated via normal phase high performance liquid chromatography (HPLC) using a Lichrospher diol-5, 4 mm \times 250 mm column and a gradient solvent system of isohexane/acetic acid (99:1) and isohexane/propan-2-ol/acetic acid (85:15:1), flow rate of 1 mL/min. Incorporation of radiolabel into TAG and DAG was analyzed

using a Radiomatic Flo-one detector (Packard, Meriden, CT) connected to the HPLC machine.

Purity of test compounds was >95%, unless otherwise indicated, as determined by HPLC methods and supported by high resolution mass spectrometry data where possible.

Synthesis methods for key compounds are given below. Experimental details for the synthesis of the rest of the compounds are available in Supporting Information.

Ethyl 6-Chloro-3,5-dimethylpyrazine-2-carboxylate (22). *Step 1. Ethyl 2-Diazo-3-oxobutanoate (19).* Polymer-bound tosyl azide (11 g, 15.4 mmol) (typical loading 1.4 mmol/g, prepared according to Green et al.)²⁷ was swollen in dry DCM (40 mL). Ethyl acetoacetate (1.0 g, 7.7 mmol, CAS 141-97-9) and triethylamine (3.2 mL, 23.1 mmol) were dissolved in DCM (10 mL) and added to the polymer containing solution. The resulting mixture was then shaken at room temperature under nitrogen until the reaction was judged completed by TLC, typically 6 h. The supernatant was filtered off. Then the resin was washed with DCM (3 × 30 mL) to rinse out residual product. The reaction mixture was evaporated to dryness to afford **19** (1.1 g, 92%) as a yellow oil. ¹H NMR (400 MHz, CDCl₃) δ 1.33 (t, *J* = 7.13 Hz, 3H), 2.48 (s, 3H), 4.30 (q, *J* = 7.13 Hz, 2H).

Typically these intermediates were not characterized because of their high energetic properties³⁰ but carried through to the following step as crude products.

Step 2. Ethyl 2-[[N-(tert-Butoxycarbonyl)-L-alanyl]amino]-3-oxobutanoate (20). Intermediate **19** (500 mg, 3.2 mmol) and Boc-L-Ala-NH₂ (843.8 mg, 4.5 mmol, CAS 85642-13-3) were added to a round bottomed flask, sealed, and back-filled with argon. Dry toluene (30 mL) was added via syringe, and the resulting heterogeneous mixture was stirred at 90 °C for 10 min to get a homogeneous solution. Meanwhile, the rhodium(II) octanoate dimer (62.3 mg, 0.080 mmol, CAS 73482-96-9) was dissolved in toluene (5 mL) and put on an ultrasound bath for 5 min to get a fine Rh dispersion. The dispersion was then added dropwise to the reaction mixture at 80 °C (a violent nitrogen effervescence was observed). After being stirred for another 20 min at elevated temperature, the reaction mixture was concentrated under reduced pressure to give a black pasty solid. The crude was purified by flash chromatography (20–80% EtOAc in heptanes) to afford **20** (850 mg, 84%) (diastereomeric mixture) as a yellow oil. ESI-MS (*m/z*): 317 (MH⁺).

Step 3. Ethyl 3,5-Dimethyl-6-oxo-1,6-dihydropyrazine-2-carboxylate (21). To a solution of **20** (800 mg, 2.53 mmol) in dry DCE (40 mL) was added TFA (1.95 mL, 25.3 mmol). The reaction mixture was heated to reflux for 4 h, and the solvent was removed under vacuum. The crude product was purified by flash chromatography (20–80% EtOAc in heptanes) to afford **21** (160 mg, 32%) as a white-yellow powder. The crude product from this reaction can optionally be used directly in the next step without purification. ¹H NMR (400 MHz, CDCl₃) δ 1.42 (t, *J* = 7.15 Hz, 3H), 2.53 (s, 3H), 2.63 (s, 3H), 4.44 (q, *J* = 7.15 Hz, 2H). ESI-MS (*m/z*): 197 (MH⁺).

Step 4. Ethyl 6-Chloro-3,5-dimethylpyrazine-2-carboxylate (22). To a suspension of **21** (0.23 g, 1.17 mmol) in butyronitrile (4 mL) was added POCl₃ (0.27 mL, 2.93 mmol). The mixture was heated to 150 °C for 10 min in the microwave oven and then allowed to cool to room temperature. To the reaction mixture was added water (2 mL). The phases were separated, and the organic layer was concentrated to dryness. The crude product was purified by flash chromatography (0.5% acetic acid in DCM) to afford **22** as a yellow oil (0.18 g, 73%). ¹H NMR (500 MHz, CDCl₃) δ 1.43 (t, *J* = 7.13 Hz, 3H), 2.68 (s, 3H), 2.78 (s, 3H), 4.45 (q, *J* = 7.13 Hz, 2H). ESI-MS (*m/z*): 215 (MH⁺).

6-Chloro-3,5-dimethylpyrazine-2-carboxamide (23). A 7 N solution of ammonia in MeOH (113 mL, 791.99 mmol) was added to intermediate **22** (3.4 g, 15.84 mmol), and the resulting suspension was stirred at room temperature for 20 h. The reaction mixture was filtered and air-dried to afford **23** as a cream solid (2.1 g, 72%). ¹H NMR (400 MHz, DMSO-*d*₆) δ 2.59 (s, 3H), 2.67 (s, 3H), 7.70 (s, 1H), 7.99 (s, 1H). ESI-MS (*m/z*): 186 (MH⁺).

tert-Butyl {trans-4-[4-(4,4,5,5-Tetramethyl-1,3,2-dioxaborolan-2-yl)phenyl]cyclohexyl}acetate (28). *Step 1: tert-Butyl [4-(4-Hydroxyphenyl)cyclohexylidene]acetate (25).* To an ice-cold solution of 4-(4-hydroxyphenyl)cyclohexanone **24** (15.22 g, 78.4 mmol, CAS 105640-07-1) in THF (375 mL) under nitrogen was added 60% sodium

hydride in mineral oil (3.28 g, 79.3 mmol) to give a thick suspension. In a separate flask 60% sodium hydride in mineral oil (4.06 g, 98.0 mmol) was suspended in dry THF (375 mL) under nitrogen. The suspension was cooled to 0 °C, and *tert*-butyl *P,P*-dimethylphosphonoacetate (16.8 mL, 82.3 mmol, CAS 62327-21-3) was added carefully. Both mixtures were stirred for ~15 min before the ice baths were removed. After 2 h at room temperature the ketone solution was transferred to the ylide solution via a syringe. The combined mixture was stirred under nitrogen overnight. The reaction was quenched by the addition of water (100 mL), and THF was then removed under vacuum. More water was added (150 mL), and the aqueous solution was extracted with EtOAc (3 × 200 mL). The combined organic layers were washed with brine (2 × 200 mL) and dried through a phase separator. Concentration gave **25** as a colorless oil (24.6 g, 99%). ¹H NMR (500 MHz, CDCl₃) δ 1.49 (s, 9H), 1.55–1.63 (m, 2H), 1.94–2.07 (m, 3H), 2.26–2.39 (m, 2H), 2.66–2.76 (m, 1H), 3.85–3.96 (m, 1H), 4.58 (s, 1H), 5.60 (s, 1H), 6.76 (d, *J* = 8.52 Hz, 2H), 7.07 (d, *J* = 8.49 Hz, 2H). ESI-MS (*m/z*): 287 (MH⁺).

Step 2: tert-Butyl [trans-4-(4-Hydroxyphenyl)cyclohexyl]acetate (26). To a solution of **25** (4.2 g, 14.56 mmol) in EtOAc (120 mL) was added 10% palladium on carbon (390 mg). The reaction was hydrogenated for 3 h (5 bar). The catalyst was filtered off through Celite, and the organic filtrate was washed with water, dried through a phase separator, and concentrated to a colorless oil (4.02 g of *cis/trans* mixture). The crude mixture was purified by chiral HPLC (neutral) using a Chiralpak AD (250 mm × 50 mm) column and 100% ACN as mobile phase to afford the desired pure *trans*-phenol **26** (2.88 g, 68%) as a white solid and also pure *cis*-phenol. NMR analysis of both isomers confirmed that the major isomer was *trans*. ¹H NMR (400 MHz, CDCl₃) δ 1.04–1.22 (m, 2H), 1.35–1.55 (m, 11H), 1.71–1.95 (m, 5H), 2.15 (d, *J* = 6.82 Hz, 2H), 2.33–2.48 (m, 1H), 4.86 (s, 1H), 6.76 (d, *J* = 8.08 Hz, 2H), 7.07 (d, *J* = 8.24 Hz, 2H). ESI-MS (*m/z*): 289 (MH⁺).

Step 3: tert-Butyl [trans-4-(4-((Trifluoromethyl)sulfonyl)oxy)phenyl]cyclohexyl]acetate (27). To a solution of **26** (2.86 g, 9.9 mmol) in DCM (75 mL) was added pyridine (1.59 mL, 19.7 mmol). The solution was cooled on an ice bath, and trifluoromethanesulfonic anhydride (1.99 mL, 11.8 mmol) was added dropwise. The ice bath was removed, and the reaction mixture was stirred for 10 min. The reaction was quenched with 1 M HCl (aq), diluted with DCM, and washed with saturated NaHCO₃ (aq) and brine. The organic layer was dried through a phase separator and concentrated. The crude product was purified by flash chromatography (8% EtOAc in heptanes) to afford **27** (4.06 g, 98%) as a white crystalline solid. ¹H NMR (500 MHz, CDCl₃) δ 1.11–1.23 (m, 2H), 1.44–1.55 (m, 11H), 1.77–1.98 (m, 5H), 2.17 (d, *J* = 7.02 Hz, 2H), 2.47–2.57 (m, 1H), 7.20 (d, *J* = 8.67 Hz, 2H), 7.28 (d, *J* = 8.67 Hz, 2H). ESI-MS (*m/z*): 421 (MH⁺).

Step 4: tert-Butyl [trans-4-[4-(4,4,5,5-Tetramethyl-1,3,2-dioxaborolan-2-yl)phenyl]cyclohexyl]acetate (28). To a suspension of PdCl₂(dppf) (0.93 g, 1.27 mmol, CAS 72287-26-4) in dioxane (135 mL) under nitrogen was added **27** (17.9 g, 42.4 mmol), triethylamine (17.7 mL, 127 mmol), and finally a 1 M solution of 4,4,5,5-tetramethyl-1,3,2-dioxaborolane in THF (72 mL, 72 mmol, CAS 25015-63-8). The mixture was refluxed for 7 h, cooled to 10 °C, and carefully quenched with water. The aqueous solution was extracted with two portions of DCM, and the combined organic layers were dried through a phase separator and concentrated to give a black oil. The crude residue was purified by flash chromatography (6% EtOAc in heptanes) to afford **28** (12.1 g, 71%) as a white powder. ¹H NMR (500 MHz, CDCl₃) δ 1.09–1.23 (m, 2H), 1.33 (s, 12H), 1.47 (s, 9H), 1.48–1.6 (m, 2H), 1.76–1.95 (m, 5H), 2.15 (d, *J* = 6.98 Hz, 2H), 2.4–2.58 (m, 1H), 7.23 (d, *J* = 7.92 Hz, 2H), 7.75 (d, *J* = 7.94 Hz, 2H).

{trans-4-[4-(6-Carbamoyl-3,5-dimethylpyrazin-2-yl)phenyl]cyclohexyl}acetic Acid (30). *Method 1. Step 1: Ethyl 6-[4-[trans-4-(2-tert-Butoxy-2-oxoethyl)cyclohexyl]phenyl]-3,5-dimethylpyrazine-2-carboxylate.* To a solution of ethyl 6-chloro-3,5-dimethylpyrazine-2-carboxylate (**22**) (0.580 g, 2.70 mmol) in DME (22 mL), EtOH (12 mL), and water (5 mL) were added boronic ester **28** (1.244 g, 3.11 mmol), potassium phosphate (tribasic) (0.688 g, 3.24 mmol), and PdCl₂(dppf) (0.119 g, 0.16 mmol). The solution was degassed with nitrogen for 10 min and then heated in the microwave oven at 140 °C for 20 min. Additional amounts of boronic ester and PdCl₂(dppf) were

added to drive the reaction. The microwave heating was continued at 140 °C for an additional 30 min. The mixtures were combined, filtered through a glass filter funnel, and evaporated. The remaining black residue was dissolved in EtOAc, washed with 0.5 M HCl (aq), and extracted with two portions of EtOAc. The combined organic layers were dried through a phase separator and concentrated to dryness. The crude compound was purified by flash chromatography (0–50% EtOAc in heptane) to afford the title compound (1.063 g, 80%) as an oil. ¹H NMR (500 MHz, CDCl₃) δ 1.12–1.22 (m, 2H), 1.42 (t, J = 7.13 Hz, 3H), 1.47 (s, 9H), 1.49–1.59 (m, 2H), 1.76–1.97 (m, 5H), 2.16 (d, J = 6.99 Hz, 2H), 2.48–2.59 (m, 1H), 2.66 (s, 3H), 2.80 (s, 3H), 4.45 (q, J = 7.12 Hz, 2H), 7.30 (d, J = 8.10 Hz, 2H), 7.52 (d, J = 8.13 Hz, 2H).

Step 2: 6-[4-[trans-4-(2-tert-butoxy-2-oxoethyl)cyclohexyl]phenyl]-3,5-dimethylpyrazine-2-carboxylic Acid. To a solution of ethyl 6-[4-[trans-4-(2-tert-butoxy-2-oxoethyl)cyclohexyl]phenyl]-3,5-dimethylpyrazine-2-carboxylate (0.530 g, 1.17 mmol) in THF (10 mL) was added LiOH (1M, 15 mL). The mixture was stirred at room temperature for 5 h. THF was removed under vacuum, and the aqueous residue was acidified with 1 M HCl (aq) and extracted with EtOAc. The organic layer was dried through a phase separator and concentrated to afford the title compound (0.5 g, 100%). ¹H NMR (400 MHz, CDCl₃) δ 1.12–1.3 (m, 2H), 1.47 (s, 9H), 1.52–1.63 (m, 2H), 1.8–2.02 (m, 5H), 2.17 (d, J = 6.89 Hz, 2H), 2.51–2.63 (m, 1H), 2.72 (s, 3H), 3.01 (s, 3H), 7.36 (d, J = 8.06 Hz, 2H), 7.51 (d, J = 8.08 Hz, 2H). ESI-MS (m/z): 425 (MH⁺).

Step 3: tert-Butyl {trans-4-[4-(6-Carbamoyl-3,5-dimethylpyrazin-2-yl)phenyl]cyclohexyl}acetate. To a solution of PyBOP (717 mg, 1.38 mmol) and NH₄Cl (196.6 mg, 3.68 mmol) in DMF (50 mL) were added 6-[4-[trans-4-(2-tert-butoxy-2-oxoethyl)cyclohexyl]phenyl]-3,5-dimethylpyrazine-2-carboxylic acid (390.0 mg, 0.92 mmol) and finally DIPEA (0.80 mL, 4.59 mmol) to initiate the reaction. The solution was stirred for 5 h at room temperature. The reaction was quenched by the addition of saturated Na₂CO₃ (aq) and extracted with toluene (3 × 100 mL). The combined organic layers were washed with brine and water, dried over Na₂SO₄, filtered, and concentrated under reduced pressure. The crude compound was purified by flash chromatography (20–60% EtOAc in petroleum ether) to afford the title compound as a white solid (376 mg, 96%). ¹H NMR (400 MHz, CDCl₃) δ 1.12–1.25 (m, 2H), 1.47 (s, 9H), 1.51–1.63 (m, 2H), 1.78–2.04 (m, 5H), 2.17 (d, J = 6.90 Hz, 2H), 2.5–2.6 (m, 1H), 2.67 (s, 3H), 2.98 (s, 3H), 7.33 (d, J = 8.13 Hz, 2H), 7.52 (d, J = 8.11 Hz, 2H), 7.80 (br s, 2H). ESI-MS (m/z): 424 (MH⁺).

Step 4: {trans-4-[4-(6-Carbamoyl-3,5-dimethylpyrazin-2-yl)phenyl]cyclohexyl}acetic Acid (30). To a solution of tert-butyl {trans-4-[4-(6-carbamoyl-3,5-dimethylpyrazin-2-yl)phenyl]cyclohexyl}acetate (363 mg, 0.86 mmol) in DCM (30 mL) was added TFA (3 mL) dropwise. The colorless solution gradually turned into a pale yellow clear solution. The reaction mixture was stirred under nitrogen at room temperature overnight. The solvent was evaporated to dryness. The crude compound was purified by flash chromatography (20–50% EtOAc in heptane + 3% formic acid) to afford 30 as a white solid, mp 220–223 °C (220 mg, 69%). ¹H NMR (500 MHz, DMSO-*d*₆) δ 1.06–1.22 (m, 2H), 1.42–1.59 (m, 2H), 1.68–1.89 (m, 5H), 2.15 (d, J = 6.93 Hz, 2H), 2.51–2.56 (m, 1H), 2.59 (s, 3H), 2.74 (s, 3H), 7.36 (d, J = 8.13 Hz, 2H), 7.61 (br s, 1H), 7.65 (d, J = 8.12 Hz, 2H), 8.00 (br s, 1H). ESI-HRMS calculated for C₂₁H₂₆N₃O₃ (MH⁺) 368.1974. Found: 368.1973.

{trans-4-[4-(6-Carbamoyl-3,5-dimethylpyrazin-2-yl)phenyl]cyclohexyl}acetic Acid (30). Method 2. **Step 1.** Methyl {trans-4-[4-(6-Carbamoyl-3,5-dimethylpyrazin-2-yl)phenyl]cyclohexyl}acetate (93a). 93a was prepared according to the procedure described for methyl {trans-4-[4-(6-carbamoyl-5-methylpyrazin-2-yl)phenyl]cyclohexyl}acetate (compound 31 step 8) from 23 (3.15 g, 16.97 mmol) and intermediate 66 (6.08 g, 16.97 mmol). The reaction mixture was heated to 80 °C, under nitrogen, and left to stir overnight for 16 h. The crude product was purified by flash silica chromatography (5–90% EtOAc in isohexane) to afford 93a (5.21 g, 81%) as a yellow solid. ¹H NMR (400 MHz, DMSO-*d*₆) δ 1.07–1.23 (m, 2H), 1.42–1.59 (m, 2H), 1.69–1.89 (m, 5H), 2.25 (d, J = 6.67 Hz, 2H), 2.49–2.56 (m, 1H), 2.58 (s, 3H), 2.73 (s, 3H), 3.60 (s, 3H), 7.35 (d, J = 8.23 Hz, 2H), 7.57

(s, 1H), 7.64 (d, J = 8.25 Hz, 2H), 7.97 (s, 1H). ESI-MS (m/z, %): 392 (MH⁺, 100). HPLC purity 100%.

Step 2. {trans-4-[4-(6-Carbamoyl-3,5-dimethylpyrazin-2-yl)phenyl]cyclohexyl}acetic Acid (30). 30 was prepared from intermediate 93a (5.2 g, 13.67 mmol) according to the procedure described for compound 31. The crude product was recrystallized from hot EtOH (250 mL) to give a yellow solid which was washed with diethyl ether (100 mL) and dried under vacuum at room temperature to give 30 (4.51 g, 90%) as a white solid. ¹H NMR (400 MHz, DMSO-*d*₆) δ 1.07–1.2 (m, 2H), 1.44–1.6 (m, 2H), 1.7–1.8 (m, 1H), 1.81–1.89 (m, 4H), 2.15 (d, J = 6.91 Hz, 2H), 2.53–2.55 (m, 1H), 2.58 (s, 3H), 2.73 (s, 3H), 7.36 (d, J = 8.24 Hz, 2H), 7.57 (s, 1H), 7.64 (d, J = 8.25 Hz, 2H), 7.97 (s, 1H), 11.99 (s, 1H). ESI-MS (m/z, %): 368 (MH⁺, 100).

{trans-4-[4-(6-Carbamoyl-5-methylpyrazin-2-yl)phenyl]cyclohexyl}acetic Acid (31). **Step 1.** Methyl 6-Hydroxy-3-methylpyrazine-2-carboxylate (63). A solution of (S)-methyl 2-(2-aminoacetamido)-3-oxobutanoate hydrochloride³¹ (62) (1.3 g, 5.79 mmol) in pyridine (58 mL) was stirred at 60 °C for 90 min. The reaction mixture was evaporated to afford crude product which was purified by flash silica chromatography (50–80% EtOAc in isohexane) to afford 63 as a yellow solid (0.340 g, 35%). ¹H NMR (400 MHz, CDCl₃) δ 2.59 (s, 3H), 3.94 (s, 3H), 8.27 (s, 1H). ESI-MS (m/z): 169 (MH⁺).

Step 2. Methyl 6-Chloro-3-methylpyrazine-2-carboxylate (64). A suspension of intermediate 63 (314 mg, 1.87 mmol) and phosphorus oxychloride (2.1 mL, 22.40 mmol) was stirred at 90 °C for 70 min. The reaction mixture was added dropwise to water (20 mL) while maintaining the temperature below 40 °C. The mixture was extracted with DCM (5 × 50 mL). The organic layer was dried over MgSO₄, filtered, and evaporated to afford a yellow oil which was purified by flash silica chromatography (0–20% EtOAc in isohexane) to afford 64 as a white solid (142 mg, 41%). ¹H NMR (400 MHz, CDCl₃) δ 2.76 (s, 3H), 3.93 (s, 3H), 8.56 (s, 1H). ESI-MS (m/z): 187 (MH⁺).

Step 3. 6-Chloro-3-methylpyrazine-2-carboxamide (65). A 7 N solution of ammonia in MeOH (5.5 mL, 38.05 mmol) was added to intermediate 64 (142 mg, 0.76 mmol), and the resulting suspension was stirred at room temperature for 4 h. The reaction mixture was evaporated to afford 65 as a white solid (109 mg, 83%). ¹H NMR (400 MHz, CDCl₃) δ 2.89 (s, 3H), 5.49 (s, 1H), 7.48 (s, 1H), 8.56 (s, 1H). ESI-MS (m/z): 170 (MH⁺).

Step 4. Methyl 2-(4-(4-Hydroxyphenyl)cyclohexylidene)acetate. Trimethyl phosphonoacetate (10.2 mL, 63.08 mmol) was added portionwise to NaH (3.15 g, 78.85 mmol, 60% mineral oil dispersion) in THF (250 mL) at 0 °C under nitrogen. The resulting suspension was stirred at room temperature for 30 min. In a separate flask, 4-(4-hydroxyphenyl)cyclohexanone (10 g, 52.57 mmol) was added portionwise to NaH (2.1 g, 52.57 mmol, 60% mineral oil dispersion) in THF (200 mL) at room temperature, and the resulting suspension was stirred at room temperature for 25 min. This was added to the mixture containing the phosphonate, and the resulting white suspension was stirred at room temperature for 18 h. The reaction mixture was quenched with water (250 mL), extracted with EtOAc (3 × 200 mL), and the organic layer was dried over MgSO₄, filtered, and evaporated to afford the title compound as a colorless waxy solid (12.9 g, 100%). ¹H NMR (400 MHz, DMSO-*d*₆) δ 1.31–1.57 (m, 2H), 1.86–2.06 (m, 3H), 2.25–2.41 (m, 2H), 2.69 (tt, J = 3.28, 11.94 Hz, 1H), 3.60 (s, 3H), 3.76–3.85 (m, 1H), 5.68 (s, 1H), 6.62–6.69 (m, 2H), 6.97–7.02 (m, 2H), 9.10 (s, 1H). ESI-MS (m/z): 245 (MH⁺).

Step 5. Methyl [trans-4-(4-Hydroxyphenyl)cyclohexyl]acetate (67) and Methyl [cis-4-(4-Hydroxyphenyl)cyclohexyl]acetate (90d). Methyl 2-(4-(4-hydroxyphenyl)cyclohexylidene)acetate (13.28 g, 53.92 mmol) and 10% palladium on carbon (1.3 g, 5.39 mmol) in EtOAc (250 mL) were stirred under an atmosphere of hydrogen at room temperature for 20 h. The reaction mixture was filtered and the filtrate concentrated under reduced pressure to provide crude product as a mix of trans and cis isomers (~4:3 ratio). The crude material was recrystallized from EtOAc (10 mL) to provide the title compound as colorless crystals (4.173g, 31%, ratio trans/cis of ~10:1).

Methyl [trans-4-(4-hydroxyphenyl)cyclohexyl]acetate (67): ¹H NMR (400 MHz, DMSO-*d*₆) δ 1.02–1.18 (m, 2H), 1.32–1.48 (m, 2H), 1.66–1.84 (m, 5H), 2.23 (d, J = 6.79 Hz, 2H), 2.33 (tt, J = 2.95,

11.92 Hz, 1H), 3.60 (s, 3H), 6.66 (d, $J = 8.39$ Hz, 2H), 7.00 (d, $J = 8.43$ Hz, 2H), 9.04 (s, 1H).

Methyl *cis*-4-(4-hydroxyphenyl)cyclohexylacetate (**90d**): ^1H NMR (400 MHz, DMSO- d_6) δ 1.51–1.64 (m, 8H), 2.14–2.19 (m, 1H), 2.44 (m, 3H), 3.60 (s, 3H), 6.67 (d, $J = 8.51$ Hz, 2H), 7.04 (d, $J = 8.48$ Hz, 2H), 9.04 (s, 1H).

Step 6. Methyl [*trans*-4-(4-[[Trifluoromethyl]sulfonyl]oxy)phenyl]cyclohexylacetate (**91a**). Trifluoromethanesulfonic anhydride (4.07 mL, 24.16 mmol) was added dropwise to a solution of intermediate **67** (5.0 g, 20.14 mmol) in DCM (100 mL) at 0 °C, and the mixture was allowed to stir at 0 °C for 20 min. Triethylamine (7.9 mL, 56.38 mmol) was added dropwise over a period of 40 min while maintaining the internal temperature under 5 °C, and after complete addition the reaction mixture was allowed to stir at 0 °C for a further 1.5 h under nitrogen. The mixture was warmed to room temperature and then quenched cautiously with water (100 mL). The organic layer was separated, the aqueous layer was reextracted with DCM (100 mL), and the combined organics were washed with saturated NaHCO_3 (75 mL) before being evaporated to afford crude product which was purified by flash silica chromatography (5–30% EtOAc in isohexane) to afford the **91a** as a colorless oil which crystallized on standing (7.27 g, 95%). ^1H NMR (400 MHz, DMSO) δ 1.05–1.22 (m, 2H), 1.38–1.55 (m, 2H), 2.24 (d, $J = 6.72$ Hz, 2H), 2.5–2.58 (m, 1H), 3.59 (s, 3H), 7.34–7.39 (m, 2H), 7.39–7.44 (m, 2H). ESI-MS (m/z , %): 379 (MH^+).

Step 7. Methyl [*trans*-4-[4-(4,4,5,5-Tetramethyl-1,3,2-dioxaborolan-2-yl)]phenyl]cyclohexylacetate (**66**). A solution of intermediate **91a** (10 g, 26.29 mmol), pinacolborane (7.34 g 28.92 mmol), KOAc (7.74 g, 78.87 mmol), dppf (0.884 g, 1.58 mmol), and $\text{Pd}(\text{dppf})\text{Cl}_2$ (1.3 g, 1.58 mmol) was degassed and heated to 80 °C for 17 h. The reaction mixture was allowed to cool and then evaporated to dryness. The residue was suspended in EtOAc and filtered through a pad of silica (~3 in. diameter \times 1 in. deep), washing through with EtOAc. The solution was evaporated to afford crude product which was purified by flash silica chromatography (0–20% EtOAc in isohexane) to afford **66** as a white solid. (7.07 g, 75%). ^1H NMR (400 MHz, DMSO- d_6) δ 1.1–1.26 (m, 2H), 1.34 (s, 12H), 1.44–1.61 (m, 2H), 1.74–1.92 (m, 5H), 2.30 (d, $J = 6.73$ Hz, 2H), 2.47–2.54 (m, 1H), 3.66 (s, 3H), 7.29 (d, $J = 8.01$ Hz, 2H), 7.65 (d, $J = 8.07$ Hz, 2H). ESI-MS (m/z , %): mass ion not observed. HPLC purity 100%.

Step 8. Methyl [*trans*-4-[4-(6-Carbamoyl-5-methylpyrazin-2-yl)]phenyl]cyclohexylacetate. A solution of intermediate **65** (109 mg, 0.64 mmol), intermediate **66** (228 mg, 0.64 mmol), and K_3PO_4 (162 mg, 0.76 mmol) in DME (10 mL), EtOH (2.5 mL), and water (2.5 mL) was degassed before addition of $\text{Pd}(\text{dppf})\text{Cl}_2$ -DCM (26.1 mg, 0.03 mmol). The reaction mixture was heated to 80 °C under nitrogen and left to stir at 80 °C for 30 min. The reaction mixture was allowed to cool to room temperature and then evaporated. The crude product was partitioned between EtOAc (70 mL) and water (30 mL), filtered through Celite, and the organic phase was separated and washed with saturated brine (50 mL). The organic layer was dried over MgSO_4 , filtered, and evaporated to afford crude product which was purified by flash chromatography (0–70% EtOAc in isohexane) to afford the title compound (194 mg, 83%) as a white solid. ^1H NMR (400 MHz, CDCl_3) δ 1.07–1.23 (m, 2H), 1.42–1.56 (m, 2H), 1.75–1.93 (m, 5H), 2.21 (d, $J = 6.69$ Hz, 2H), 2.44–2.55 (m, 1H), 2.94 (s, 3H), 3.62 (s, 3H), 5.47 (s, 1H), 7.29 (d, $J = 8.22$ Hz, 2H), 7.80 (s, 1H), 7.85 (d, $J = 8.36$ Hz, 2H), 8.95 (s, 1H). ESI-MS (m/z): 368 (MH^+).

Step 9. [*trans*-4-[4-(6-Carbamoyl-5-methylpyrazin-2-yl)]phenyl]cyclohexylacetic Acid (**31**). Powdered KOH (89 mg, 1.58 mmol) was added in one portion to methyl [*trans*-4-[4-(6-carbamoyl-5-methylpyrazin-2-yl)]phenyl]cyclohexylacetate (194 mg, 0.53 mmol) in *t*-BuOH (5 mL) at 45 °C. The resulting solution was stirred at 45 °C for 150 min, and a thick white suspension slowly formed. Then 1 N citric acid (5 mL) was added. The mixture was evaporated to remove the organic solvent, and the suspension was filtered and dried to give a white solid. The crude product was purified by preparative HPLC (Waters XBridge Prep C18 OBD column, 5 μm silica, 50 mm diameter, 150 mm length) (5–95% MeCN in H_2O (containing 0.1% formic acid)) to afford **31** as a white solid (120 mg, 64%). ^1H NMR (400 MHz, DMSO- d_6) δ 0.99–1.14 (m, 2H), 1.37–1.52 (m, 2H), 1.64–1.8 (m, 4H), 2.07 (d, $J = 6.90$ Hz, 2H),

2.43–2.54 (m, 1H), 2.68 (s, 3H), 7.31 (d, $J = 8.36$ Hz, 2H), 7.62 (s, 1H), 8.07 (d, $J = 8.39$ Hz, 2H), 8.14 (s, 1H), 9.11 (s, 1H), 11.89 (s, 1H). ESI-MS (m/z): 352 (MH^+). ESI-HRMS calculated for $\text{C}_{20}\text{H}_{24}\text{N}_3\text{O}_3$ (MH^+) 354.181 22; found, 354.181 05. HPLC purity 100%.

3,5-Dimethyl-6-[4-[*trans*-4-(1H-tetrazol-5-ylmethyl)cyclohexyl]phenyl]pyrazine-2-carboxamide (60). **Step 1:** Ethyl 6-[4-[*trans*-4-(2-Cyanoethylcarbamoyl)cyclohexyl]phenyl]-3,5-dimethylpyrazine-2-carboxylate. Ethyl 6-[4-[*trans*-4-(2-*tert*-butoxy-2-oxoethyl)cyclohexyl]phenyl]-3,5-dimethylpyrazine-2-carboxylate (see compound **30**, method 1, step 1) (300 mg, 0.66 mmol) was dissolved in DCM (20 mL), and TFA (2 mL) was added dropwise. The mixture was stirred at room temperature for 16 h and then concentrated to dryness to give the liberated carboxylic acid. The acid (250 mg, 0.63 mmol) was dissolved in DCM (20 mL), and 2-cyanoethylamine (66.3 mg, 0.95 mmol), DIPEA (0.22 mL, 1.3 mmol), and PyBOP (492 mg, 0.95 mmol) were added in one portion. The resulting mixture was stirred at room temperature for 5 h. The crude compound was purified by flash chromatography (95% EtOAc in pentane) to afford the title compound (267 mg, 0.60 mmol). ESI-MS (m/z): 449 (MH^+).

Step 2: 6-[4-[*trans*-4-(1H-Tetrazol-5-ylmethyl)cyclohexyl]phenyl]-3,5-dimethylpyrazine-2-carboxylic Acid. The 2-cyanoamide (240 mg, 0.54 mmol) from the previous step was dissolved in THF (10 mL). Then DEAD (699 mg, 1.61 mmol), triphenylphosphine (421 mg, 1.61 mmol), and trimethylsilyl azide (184.9 mg, 1.61 mmol) were added. The reaction mixture was stirred at room temperature for 16 h under nitrogen atmosphere. Then another equivalent of DEAD, triphenylphosphine, and trimethylsilyl azide was added and the reaction mixture was stirred for another 16 h and evaporated to dryness. The crude was dissolved in THF (10 mL) and water (1 mL). Then LiOH (51 mg, 2.14 mmol) was added. The mixture was stirred for 16 h, acidified to pH 1 using 3 M HCl (aq), and extracted with DCM (3 \times 50 mL). The organic layers were dried using Na_2SO_4 and evaporated to dryness to afford the title compound. ESI-MS (m/z): 392.9 (MH^+).

Step 3: 3,5-Dimethyl-6-[4-[*trans*-4-(1H-tetrazol-5-ylmethyl)cyclohexyl]phenyl]pyrazine-2-carboxamide (**60**). This compound was synthesized from the carboxylic acid from a previous step using a similar protocol for amide coupling as described for compound **30** (step 3) to afford **60** as a white solid, mp 208–209 °C. (32 mg, 35%). ^1H NMR (600 MHz, CD_3OD) δ 1.23–1.36 (m, 2H), 1.51–1.67 (m, 2H), 1.87–2 (m, 5H), 2.56–2.67 (m, 4H), 2.85 (s, 3H), 2.92 (d, $J = 6.97$ Hz, 2H), 7.37 (d, $J = 8.15$ Hz, 2H), 7.58 (d, $J = 8.16$ Hz, 2H). ESI-HRMS calculated for $\text{C}_{21}\text{H}_{25}\text{N}_7\text{O}$ (MH^+), 392.2199. Found: 392.2188.

[*trans*-5'-(6-Carbamoyl-3,5-dimethylpyrazin-2-yl)-2',3'-dihydrospiro[cyclohexane-1,1'-inden]-4-yl]acetic Acid (78). **Step 1.** (5-Bromo-2,3-dihydro-1H-inden-1-ylidene)methyl Methyl Ether (**95**). (Methoxymethyl)triphenylphosphonium chloride (41.1 g, 120 mmol) was added to a stirred suspension of potassium *tert*-butoxide (13.46 g, 120 mmol) in 1,4-dioxane (224 mL) at room temperature over a period of 10 min under nitrogen. The resulting red solution was stirred at room temperature for 2 h, and then a solution of 5-bromo-1-indanone (11 g, 52.17 mmol) in 1,4-dioxane (126 mL) was added over a period of 10 min under nitrogen. The resulting solution was stirred at room temperature for 3 h and then allowed to stand over the weekend. The reaction mixture was poured into water (500 mL), extracted with EtOAc (2 \times 500 mL), and the organic layer was washed with saturated brine (300 mL), dried over MgSO_4 , filtered, and evaporated to afford a black oil. To the crude oil were added EtOAc and isohexane (1:2, 400 mL) to give a solid which was collected by filtration and washed with EtOAc and isohexane (200 mL). The filtrate was evaporated to afford crude product which was purified by flash silica chromatography (0–5% EtOAc in isohexane) to afford **95** as a yellow oil (9.96 g, 80%). ^1H NMR (400 MHz, CDCl_3) δ 2.64–2.71 (m, 1H), 2.71–2.79 (m, 1H), 2.9–2.99 (m, 2H), 3.72 (s, 3H), 6.62 (t, $J = 2.57$ Hz, 1H), 7.10 (d, $J = 8.22$ Hz, 1H), 7.27–7.35 (m, 2H).

Step 2. 5'-Bromo-2',3'-dihydro-4H-spiro[cyclohex-2-ene-1,1'-inden]-4-one (**96**). Methyl vinyl ketone (2.9 mL, 35.88 mmol) was added to a stirred mixture of **95** (4.29 g, 17.94 mmol) and *p*-toluenesulfonic acid monohydrate (3.41 g, 17.94 mmol) in toluene (20 mL), and the resulting mixture was stirred at 100 °C for 6 h and then allowed to cool to ambient temperature overnight. The mixture was poured into saturated NaHCO_3 (75 mL), extracted with EtOAc (3 \times 200 mL), and

the combined organic extracts were dried over MgSO_4 , filtered, and evaporated to afford crude product which was purified by flash silica chromatography (10% EtOAc in isohexane) to afford **96** as a pale yellow solid (2.78 g, 56%). $^1\text{H NMR}$ (400 MHz, DMSO) δ 1.73–1.83 (m, 2H), 2.01 (td, $J = 4.54, 13.37$ Hz, 2H), 2.16–2.26 (m, 4H), 2.58 (td, $J = 6.12, 14.30$ Hz, 2H), 2.93 (t, $J = 7.32$ Hz, 2H), 7.20 (d, $J = 8.10$ Hz, 1H), 7.28–7.35 (m, 1H), 7.39–7.43 (m, 1H). EI-MS (m/z) 278, 280 (M^{+})

Step 3. *5'-Bromo-2',3'-dihydro-4H-spiro[cyclohexane-1,1'-inden]-4-one (97)*. 10% palladium on carbon (270 mg, 2.54 mmol) was added to a solution of **96** (2.7 g, 9.74 mmol) in acetic acid (25 mL). The mixture was evacuated with hydrogen and allowed to stir under an atmosphere of hydrogen at room temperature for 4 h. The reaction mixture was diluted with DCM (150 mL) and filtered through Celite, washing with DCM (150 mL), and the filtrate was evaporated to afford **97** as a yellow solid (2.290 g, 84%). $^1\text{H NMR}$ (400 MHz, CDCl_3) δ 1.87–1.96 (m, 3H), 2.04 (td, $J = 4.84, 13.39$ Hz, 2H), 2.24 (t, $J = 7.32$ Hz, 2H), 2.4–2.6 (m, 6H), 2.99 (t, $J = 7.32$ Hz, 2H), 7.00 (d, $J = 8.08$ Hz, 1H), 7.29–7.34 (m, 2H), 7.38 (d, $J = 1.39$ Hz, 1H). HPLC purity 93.84%.

Step 4. *tert-Butyl (5'-Bromo-2',3'-dihydro-4H-spiro[cyclohexane-1,1'-inden]-4-ylidene)acetate (98)*. To a solution of *tert*-butyl diethylphosphonoacetate (8.8 mL, 37.47 mmol) in THF (100 mL) was added 60% w/w sodium hydride (1.5 g, 37.47 mmol). The reaction mixture was stirred at room temperature for 30 min. A solution of **97** in THF (50 mL) was added, and stirring continued at room temperature for 1 h. The reaction mixture was quenched with saturated brine (150 mL), extracted with EtOAc (2 \times 200 mL), and the organic layer was dried over Na_2SO_4 , filtered, and evaporated to afford the crude product as a brown oil (13.7 g). The crude oil was triturated with isohexane to give a solid which was collected by filtration and dried under vacuum to give **98** as a beige solid (7.26 g, 62%). $^1\text{H NMR}$ (400 MHz, DMSO- d_6) δ 1.49 (s, 9H), 1.6–1.82 (m, 4H), 2.08–2.22 (m, 3H), 2.26–2.48 (m, 2H), 2.95 (t, $J = 7.33$ Hz, 2H), 3.73 (d, $J = 14.39$ Hz, 1H), 5.67 (s, 1H), 7.20 (d, $J = 8.12$ Hz, 1H), 7.32–7.38 (m, 1H), 7.44–7.46 (m, 1H). HPLC purity 100%.

Step 5. *tert-Butyl [5'-(4,4,5,5-Tetramethyl-1,3,2-dioxaborolan-2-yl)-2',3'-dihydro-4H-spiro[cyclohexane-1,1'-inden]-4-ylidene]acetate (99)*. Bis(pinacolato)diboron (6.11 g, 24.05 mmol), potassium acetate (5.67 g, 57.72 mmol), and 1,1'-bis(diphenylphosphino)ferrocene (0.539 g, 0.96 mmol) were added to a solution of **98** (7.26 g, 19.24 mmol) in dioxane (150 mL). The reaction mixture was degassed and 1,1'-bis(diphenylphosphino)ferrocene dichloropalladium(II) (0.791 g, 0.96 mmol) added. The reaction mixture was heated to 80 °C overnight. The reaction mixture was allowed to cool and then evaporated. The residue was suspended in EtOAc and filtered through a pad of silica gel, washing through with EtOAc. The filtrate was evaporated to a brown oil (12g) which was purified by flash silica chromatography (elution gradient of 0–10% EtOAc in isohexane) to afford **99** as a solid (5.42 g, 66%). $^1\text{H NMR}$ (400 MHz, DMSO- d_6) δ 1.27 (s, 12H), 1.42 (s, 9H), 1.6–1.77 (m, 4H), 2.01–2.18 (m, 3H), 2.21–2.42 (m, 2H), 2.87 (t, $J = 7.31$ Hz, 2H), 3.66 (d, $J = 14.43$ Hz, 1H), 5.74 (s, 1H), 7.17 (d, $J = 7.56$ Hz, 1H), 7.46 (d, $J = 7.51$ Hz, 1H), 7.50 (s, 1H). ESI-MS (m/z , %): 423 (MH^+ , 100). HPLC purity 100%.

Step 6. *tert-Butyl [trans-5'-(4,4,5,5-Tetramethyl-1,3,2-dioxaborolan-2-yl)-2',3'-dihydrospiro[cyclohexane-1,1'-inden]-4-yl]acetate (100)*. To a solution of **99** (5.42 g, 12.77 mmol) in tetrahydrofuran (125 mL), under nitrogen, was added 10% (w/w) palladium on carbon (1.359 g, 1.28 mmol). The atmosphere was replaced with hydrogen and the mixture stirred at room temperature for 17 h. The reaction mixture was filtered and evaporated to a colorless oil. This was dissolved in methanol (~20 mL) and cooled in a dry ice/acetone bath to produce a white solid. The suspension was allowed to warm and then evaporated to give the crude product as a white solid. This was recrystallized by dissolving in DCM (~20 mL), adding methanol (~20 mL), and cooling in a dry ice/acetone bath. The resultant suspension was filtered and the collected solid dried to give **100** as a white solid (2.290 g, 42%). $^1\text{H NMR}$ (400 MHz, DMSO- d_6) δ 1.19–1.31 (m, 2H), 1.33 (s, 12H), 1.47 (s, 9H), 1.49–1.55 (m, 2H), 1.6–1.75 (m, 4H), 1.76–1.84 (m, 1H), 1.97 (t, $J = 7.37$ Hz, 2H), 2.19 (d, $J = 6.91$ Hz, 2H), 2.87 (t, $J = 7.31$ Hz, 2H), 7.24 (d, $J = 7.48$ Hz, 1H), 7.51–7.56 (m, 2H). HPLC purity 100%.

Step 7. *tert-Butyl [trans-5'-(6-Carbamoyl-3,5-dimethylpyrazin-2-yl)-2',3'-dihydrospiro[cyclohexane-1,1'-inden]-4-yl]acetate (101)*. Acetonitrile (7 mL) was added to 1,1-bis(di-*tert*-butylphosphino)ferrocenepalladium dichloride (0.093 g, 0.16 mmol), and the mixture was stirred at room temperature for 5 min before addition of potassium carbonate (0.871 g, 6.30 mmol), water (7 mL), and **100** (1.3 g, 3.15 mmol). After a further 5 min **23** (0.585 g, 3.15 mmol) was added and the reaction mixture heated to 80 °C for 17 h. The acetonitrile was evaporated and the resultant suspension partitioned between EtOAc (50 mL) and brine (50 mL). The organic phase was dried (Na_2SO_4) and evaporated to a dark brown oil, which was purified by flash silica chromatography (elution gradient of 0–60% EtOAc in isohexane) to afford **101** as a solid (1.26 g, 89%). $^1\text{H NMR}$ (400 MHz, DMSO- d_6) δ 1.15–1.29 (m, 2H), 1.41 (s, 9H), 1.49–1.58 (m, 2H), 1.6–1.7 (m, 4H), 1.73–1.82 (m, 1H), 1.97 (t, $J = 7.36$ Hz, 2H), 2.14 (d, $J = 6.91$ Hz, 2H), 2.57 (s, 3H), 2.73 (s, 3H), 2.89 (t, $J = 7.30$ Hz, 2H), 7.29 (d, $J = 7.86$ Hz, 1H), 7.48 (dd, $J = 1.62, 7.85$ Hz, 1H), 7.52–7.54 (m, 1H), 7.57 (s, 1H), 7.96 (s, 1H). ESI-MS (m/z , %): 450 (MH^+ , 100). HPLC purity 100%.

Step 8. *[trans-5'-(6-Carbamoyl-3,5-dimethylpyrazin-2-yl)-2',3'-dihydrospiro[cyclohexane-1,1'-inden]-4-yl]acetic Acid (78)*. A solution of **101** (1.16 g, 2.58 mmol) in trifluoroacetic acid (12 mL) was allowed to stand at room temperature for 30 min. The reaction mixture was evaporated to a solid which was purified by recrystallization from MeOH to afford **78** as a white crystalline solid (0.648 g, 64%). $^1\text{H NMR}$ (300 MHz, DMSO- d_6) δ 1.12–1.31 (m, 2H), 1.47–1.59 (m, 2H), 1.59–1.86 (m, 5H), 1.98 (t, $J = 7.30$ Hz, 2H), 2.17 (d, $J = 6.79$ Hz, 2H), 2.58 (s, 3H), 2.73 (s, 3H), 2.90 (t, $J = 7.26$ Hz, 2H), 7.30 (d, $J = 7.85$ Hz, 1H), 7.50 (d, $J = 7.82$ Hz, 1H), 7.54 (s, 1H), 7.62 (s, 1H), 8.01 (s, 1H), 12.05 (s, 1H). ESI-MS (m/z , %): 394 (MH^+ , 100). ESI-HRMS calculated for $\text{C}_{23}\text{H}_{28}\text{N}_3\text{O}_3$ (MH^+) 394.21252; found, 394.21225. HPLC purity 100%.

■ ASSOCIATED CONTENT

📄 Supporting Information

Experimental details for the synthesis of compounds **12**, **13**, **18**, **29**, **32–59**, **61**, **73–77**, **79–85**, **120**. This material is available free of charge via the Internet at <http://pubs.acs.org>.

■ AUTHOR INFORMATION

Corresponding Author

*Phone: +46-31-7064308. Fax: +46-31-7763700. E-mail: petra.johannesson@astrazeneca.com.

Notes

The authors declare no competing financial interest.

■ ACKNOWLEDGMENTS

Usha Chauhan is thanked for her skillful generation of enzyme inhibition data. Martin Packer is thanked for computational input into the design of the pyrazinecarboxamide system.

■ ABBREVIATIONS USED

ACAT, acyl-coenzyme A:cholesterol acyltransferase; b.i.d., “bis in die” latin for twice a day; CL_{int} intrinsic clearance; DAG, diacylglycerol; DIAD, diisopropyl azodicarboxylate; DGAT, diacylglycerol acyltransferase; DIPEA, *N,N*-diisopropylethylamine; DMEM, Dulbecco's modified Eagle medium; Dppf, 1,1'-bis(diphenylphosphino)ferrocene; Dtbpf, 1,1'-bis(di-*tert*-butylphosphino)ferrocene; FCS, fetal calf serum; GLP-1, glucagon-like peptide 1; HATU, *O*-(7-azabenzotriazol-1-yl)-*N,N,N',N'*-tetramethyluronium hexafluorophosphate; LLE, ligand lipophilicity efficiency; log *D*, logarithm of distribution coefficient; MDCK, Madin–Darby canine kidney; OLTT, oral lipid tolerance test; Oxone, potassium peroxomonosulfate; (PinB)₂, bis(pinacolato)diboron; PyBOP, benzotriazol-1-yloxy-tripyrrolidinophosphonium hexafluorophosphate; PyBroP, bromo-tris-pyrrolidinophosphonium hexafluorophosphate;

Rh₂Oct₄, rhodium(II) octanoate dimer; SEM, standard error of the mean; TAG, triacylglycerol; TBTU, O-(benzotriazol-1-yl)-N,N,N',N'-tetramethyluronium tetrafluoroborate; TMSN₃, trimethylsilyl azide

REFERENCES

- (1) Birch, A. M.; Buckett, L. K.; Turnbull, A. V. DGAT1 inhibitors as anti-obesity and anti-diabetic agents. *Curr. Opin. Drug Discovery Dev.* **2010**, *13*, 489–496.
- (2) Zhao, G.; Souers, A. J.; Voorbach, M.; Falls, H. D.; Droz, B.; Brodjian, S.; Lau, Y. Y.; Iyengar, R. R.; Gao, J.; Judd, A. S.; Wagaw, S. H.; Ravn, M. M.; Engstrom, K. M.; Lynch, J. K.; Mulhern, M. M.; Freeman, J.; Dayton, B. D.; Wang, X.; Grihalde, N.; Fry, D.; Beno, D. W. A.; Marsh, K. C.; Su, Z.; Diaz, G. J.; Collins, C. A.; Sham, H.; Reilly, R. M.; Brune, M. E.; Kym, P. R. Validation of diacyl glycerol acyltransferase I as a novel target for the treatment of obesity and dyslipidemia using a potent and selective small molecule inhibitor. *J. Med. Chem.* **2008**, *51*, 380–383.
- (3) Birch, A. M.; Birtles, S.; Buckett, L. K.; Kemmitt, P. D.; Smith, G. J.; Smith, T. J. D.; Turnbull, A. V.; Wang, S. J. Y. Discovery of a potent, selective, and orally efficacious pyrimidinooxazinyl bicyclooctaneacetic acid diacylglycerol acyltransferase-1 inhibitor. *J. Med. Chem.* **2009**, *52*, 1558–1568.
- (4) Fox, B. M.; Iio, K.; Li, K.; Choi, R.; Inaba, T.; Jackson, S.; Sagawa, S.; Shan, B.; Tanaka, M.; Yoshida, A.; Kayser, F. Discovery of pyrrolopyridazines as novel DGAT1 inhibitors. *Bioorg. Med. Chem. Lett.* **2010**, *20*, 6030–6033.
- (5) Nakada, Y.; Aicher, T. D.; Le Huerou, Y.; Turner, T.; Pratt, S. A.; Gonzales, S. S.; Boyd, S. A.; Miki, H.; Yamamoto, T.; Yamaguchi, H.; Kato, K.; Kitamura, S. Novel acyl coenzyme A (CoA): diacylglycerol acyltransferase-1 inhibitors: synthesis and biological activities of diacylethylenediamine derivatives. *Bioorg. Med. Chem.* **2010**, *18*, 2785–2795.
- (6) Nakada, Y.; Ogino, M.; Asano, K.; Aoki, K.; Miki, H.; Yamamoto, T.; Kato, K.; Masago, M.; Tamura, N.; Shimada, M. Novel acyl coenzyme A: diacylglycerol acyltransferase 1 inhibitors—synthesis and biological activities of N-(substituted heteroaryl)-4-(substituted phenyl)-4-oxobutanamides. *Chem. Pharm. Bull.* **2010**, *58*, 673–679.
- (7) Dow, R. L.; Andrews, M.; Aspnes, G. E.; Balan, G.; Michael Gibbs, E.; Guzman-Perez, A.; Karki, K.; LaPerle, J. L.; Li, J.; Litchfield, J.; Munchhof, M. J.; Perreault, C.; Patel, L. Design and synthesis of potent, orally-active DGAT-1 inhibitors containing a dioxino[2,3-d]pyrimidine core. *Bioorg. Med. Chem. Lett.* **2011**, *21*, 6122–6125.
- (8) Dow, R. L.; Li, J.; Pence, M. P.; Gibbs, E. M.; LaPerle, J. L.; Litchfield, J.; Piotrowski, D. W.; Munchhof, M. J.; Manion, T. B.; Zavadoski, W. J.; Walker, G. S.; McPherson, R. K.; Tapley, S.; Sugarman, E.; Guzman-Perez, A.; DaSilva-Jardine, P. Discovery of PF-04620110, a potent, selective, and orally bioavailable inhibitor of DGAT-1. *ACS Med. Chem. Lett.* **2011**, *2*, 407–412.
- (9) Motiwala, H.; Kandre, S.; Birar, V.; Kadam, K. S.; Rodge, A.; Jadhav, R. D.; Mahesh Kumar Reddy, M.; Brahma, M. K.; Deshmukh, N. J.; Dixit, A.; Doshi, L.; Gupte, A.; Gangopadhyay, A. K.; Vishwakarma, R. A.; Srinivasan, S.; Sharma, M.; Nemmani, K. V. S.; Sharma, R. Exploration of pyridine containing heteroaryl analogs of biaryl ureas as DGAT1 inhibitors. *Bioorg. Med. Chem. Lett.* **2011**, *21*, 5812–5817.
- (10) Qian, Y.; Wertheimer, S. J.; Ahmad, M.; Cheung, A. W.; Firooznia, F.; Hamilton, M. M.; Hayden, S.; Li, S.; Marcopulos, N.; McDermott, L.; Tan, J.; Yun, W.; Guo, L.; Pamidimukkala, A.; Chen, Y.; Huang, K.; Ramsey, G. B.; Whittard, T.; Conde-Knape, K.; Taub, R.; Rondinone, C. M.; Tilley, J.; Bolin, D. Discovery of orally active carboxylic acid derivatives of 2-phenyl-5-trifluoromethylloxazole-4-carboxamide as potent diacylglycerol acyltransferase-1 inhibitors for the potential treatment of obesity and diabetes. *J. Med. Chem.* **2011**, *54*, 2433–2446.
- (11) Bali, U.; Barba, O.; Dawson, G.; Gattrell, W. T.; Horswill, J. G.; Pan, D. A.; Procter, M. J.; Rasamison, C. M.; Sambrook Smith, C. P.; Taylor-Warne, A.; Wong-Kai-In, P. Design and synthesis of potent carboxylic acid DGAT1 inhibitors with high cell permeability. *Bioorg. Med. Chem. Lett.* **2012**, *22*, 824–828.
- (12) Mougnot, P.; Namane, C.; Fett, E.; Camy, F.; Dadi-Faihun, R.; Langot, G.; Monseu, C.; Onofri, B.; Pacquet, F.; Pascal, C.; Crespin, O.; Ben-Hassine, M.; Ragot, J. L.; Van-Pham, T.; Philippo, C.; Chatelain-Egger, F.; Peron, P.; Le Bail, J. C.; Guillot, E.; Chamiot-Clerc, P.; Chabanaud, M.; Pruniaux, M.; Schmidt, F.; Venier, O.; Nicolai, E.; Viviani, F. Thiadiazoles as new inhibitors of diacylglycerol acyltransferase type 1. *Bioorg. Med. Chem. Lett.* **2012**, *22*, 2497–2502.
- (13) Serrano-Wu, M. H.; Coppola, G. M.; Gong, Y.; Neubert, A. D.; Chatelain, R.; Clairmont, K. B.; Commerford, R.; Cosker, T.; Daniels, T.; Hou, Y.; Jain, M.; Juedes, M.; Li, L.; Mullarkey, T.; Rocheford, E.; Sung, M. J.; Tyler, A.; Yang, Q.; Yoon, T.; Hubbard, B. K. Intestinally targeted diacylglycerol acyltransferase 1 (DGAT1) inhibitors robustly suppress postprandial triglycerides. *ACS Med. Chem. Lett.* **2012**, *5*, 411–415.
- (14) McCoull, W.; Addie, M. S.; Birch, A. M.; Birtles, S.; Buckett, L. K.; Butlin, R. J.; Bowker, S. S.; Boyd, S.; Chapman, S.; Davies, R. D. M.; Donald, C. S.; Green, C. P.; Jenner, C.; Kemmitt, P. D.; Leach, A. G.; Moody, G. C.; Morentin Gutierrez, P.; Newcombe, N. J.; Nowak, T.; Packer, M. J.; Plowright, A. T.; Revill, J.; Schofield, P.; Sheldon, C.; Stokes, S.; Turnbull, A. V.; Wang, S. J. Y.; Whalley, D. P.; Wood, J. M. Identification, optimisation and in vivo evaluation of oxadiazole DGAT-1 inhibitors for the treatment of obesity and diabetes. *Bioorg. Med. Chem. Lett.* **2012**, *22*, 3873–3878.
- (15) Yeh, V. S. C.; Beno, D. W. A.; Brodjian, S.; Brune, M. E.; Cullen, S. C.; Dayton, B. D.; Dhaon, M. K.; Falls, H. D.; Gao, J.; Grihalde, N.; Hajduk, P.; Hansen, T. M.; Judd, A. S.; King, A. J.; Klir, R. C.; Larson, K. J.; Lau, Y. Y.; March, K. C.; Mittelstadt, S. W.; Plata, D.; Rozema, M. J.; Segreti, J. A.; Stoner, E. J.; Voorbach, M. J.; Wang, X.; Xin, X.; Zhao, G.; Collins, C. A.; Cox, B. F.; Reilly, R. M.; Kym, P. R.; Souers, A. J. Identification and preliminary characterization of a potent, safe, and orally efficacious inhibitor of acyl-CoA:diacylglycerol acyltransferase 1. *J. Med. Chem.* **2012**, *55*, 1751–1757.
- (16) Plowright, A. T.; Barton, P.; Bennet, S.; Birch, A. B.; Birtles, S.; Buckett, L. K.; Butlin, R.; Davies, R. D. M.; Ertan, A.; Morrentin Gutierrez, P.; Kemmit, P. D.; Leach, A. G.; Svensson, P. H.; Turnbull, A. V.; Waring, M. J. Design and synthesis of a novel series of cyclohexoxy-pyridyl derivatives as inhibitors of diacylglycerol acyl transferase 1. *MedChemComm* [Online early access]. DOI: 10.1039/c2md20187a. Published Online: August 17, 2012.
- (17) Meyers, C.; Serrano-Wu, M. H.; Thuren, T. Uses of Diacylglycerol Acyltransferase-1 (DGAT1) Inhibitors for the Treatment of Diseases or Conditions Associated with Hypertriglyceridemia WO 2011/123401, 2011.
- (18) <http://clinicaltrials.gov/ct2/show/NCT01146522?term%BCLCQ-908&%BC1>.
- (19) Waring, M. J. Lipophilicity in drug discovery. *Expert Opin. Drug Discovery* **2010**, *5*, 235–248.
- (20) Waring, M. J. Defining optimum lipophilicity and molecular weight ranges for drug candidates—molecular weight dependent lower log D limits based on permeability. *Bioorg. Med. Chem. Lett.* **2009**, *19*, 2844–2851.
- (21) Nakayama, S.; Atsumi, R.; Takakusa, H.; Kobayashi, Y.; Kurihara, A.; Nagai, Y.; Nakai, D.; Okazaki, O. A zone classification system for risk assessment of idiosyncratic drug toxicity using daily dose and covalent binding. *Drug Metab. Dispos.* **2009**, *37*, 1970–1977.
- (22) Smith, R.; Campbell, A.; Coish, P.; Dai, M.; Jenkins, S.; Lowe, D.; O'Connor, S.; Su, N.; Wang, G.; Zhang, M.; Zhu, L. Preparation and Use of Aryl Alkyl Acid Derivatives for the Treatment of Obesity. US2004/0224997A1, 2004.
- (23) Fox, B. M.; Furukawa, N.; Hao, X.; Iio, K.; Inaba, T.; Jackson, S. M.; Kayser, F.; Labelle, M.; Li, K.; Matsui, T.; McMinn, D. L.; Ogawa, N.; Rubenstein, S. M.; Sagawa, S.; Sugimoto, K.; Suzuki, M.; Tanaka, M.; Ye, G.; Yoshida, A.; Zhang, J. Fused Bicyclic Nitrogen Containing Heterocycles. WO2004/047755, 2004.
- (24) Berggren, A. I. K.; Bostrom, S. J.; Elebring, S. T.; Greasley, P.; Terricabras, E.; Wilstermann, J. M. 5,6-Diarylpyrazine-2-amide Derivatives as CB1 Antagonists. WO2003/051851, 2003.
- (25) Pappo, D.; Vartanian, M.; Lang, S.; Kashman, Y. Synthesis of cyclic endiamino peptides. *J. Am. Chem. Soc.* **2005**, *127*, 7682–7683.

(26) Matsushita, H.; Lee, S.; Yoshida, K.; Clapham, B.; Koch, G.; Zimmermann, J.; Janda, K. D. N–H insertion reactions of Boc-amino acid amides: solution- and solid-phase synthesis of pyrazinones and pyrazines. *Org. Lett.* **2004**, *6*, 4627–4629.

(27) Green, G. M.; Peet, N. P.; Metz, W. A. Polystyrene-supported benzenesulfonyl azide: a diazo transfer reagent that is both efficient and safe. *J. Org. Chem.* **2001**, *66*, 7930.

(28) Stachulski, A. V.; Harding, J. R.; Lindon, J. C.; Maggs, J. L.; Park, B. K.; Wilson, I. D. Acyl glucuronides: biological activity, chemical reactivity, and chemical synthesis. *J. Med. Chem.* **2006**, *49*, 6931–6945.

(29) Coleman, R. A. Diacylglycerol acyltransferase and monoacylglycerol acyltransferase from liver and intestine. *Methods Enzymol.* **1992**, *209*, 98–104.

(30) Clark, J. D.; Shah, A. S.; Peterson, J. C.; Patelis, L.; Kersten, R. J. A.; Heemskerk, A. H. Detonation properties of ethyl diazoacetate. *Thermochim. Acta* **2002**, *386*, 73–79.

(31) Bauer, U. A.; Birch, A. M.; Butlin, R. J.; Green, C.; Barlind, J. G.; Hovland, R.; Johannesson, P.; Johansson, J. M.; Leach, A.; Noeske, A. T.; Petersson, A. U. Carbamoyl Compounds as DGAT1 Inhibitors. WO2009/081195, 2009.